

Electronic Supplementary Information

**Ruthenocycles of benzothiazolyl and pyridyl hydrazones with ancillary PAHs:
Synthesis, structure, electrochemistry and antimicrobial activity**

Soumitra Dinda^{a,†}, Tamanna Sultana^{a,‡}, Suhana Sultana^{a,‡}, Sarat Chandra Patra^b, Arup Kumar Mitra^{a,‡},
Subhadip Roy^c, Kausikisankar Pramanik^{b,*} and Sanjib Ganguly^{a,†*}

^{a, †}Department of Chemistry, St. Xavier's College (Autonomous), Kolkata – 700016, India

^{a, ‡}Department of Microbiology, St. Xavier's College (Autonomous), Kolkata – 700016, India

^bDepartment of Chemistry, Jadavpur University, India.

^cDepartment of Chemistry, The ICFAI University Tripura, Tripura 799210, India

*To whom correspondence should be addressed. icsgxav@gmail.com; icsg@sxccal.edu Tel: +91 33 2255

Table S1 Crystallographic data and structure refinement for **3a**, **3b**, **3c** and **4b**

Identification code	3a	3b	3c	4b
Empirical formula	C ₅₉ H ₄₄ ClN ₃ OP ₂ Ru	C ₅₃ H ₄₂ ClN ₃ OP ₂ Ru	C ₅₃ H ₄₂ ClN ₃ OP ₂ Ru	C ₅₆ Cl ₃ H ₄₄ N ₃ OP ₂ RuS
Formula weight	1009.491	935.409	935.409	1076.429
Temperature/K	273.15	300.0	298.43	298.14
Crystal system	triclinic	triclinic	monoclinic	triclinic
Space group	<i>P</i> -1	<i>P</i> -1	<i>P</i> 2 ₁ /n	<i>P</i> -1
a/Å	10.4963(8)	12.7697(15)	20.496(1)	12.5638(7)
b/Å	13.4855(11)	14.3912(17)	10.4384(5)	14.5528(8)
c/Å	18.0538(14)	14.5106(18)	22.9609(11)	30.3087(16)
α/°	107.300(2)	103.662(5)	90	78.061(2)
β/°	93.585(2)	113.280(4)	114.403(2)	78.123(2)
γ/°	103.021(2)	103.410(5)	90	67.430(2)
Volume/Å ³	2354.0(3)	2216.6(5)	4473.5(4)	4957.2(5)
Z	2	2	4	4
ρ _{calcg/cm³}	1.424	1.402	1.389	1.442
μ/mm ⁻¹	0.504	0.529	0.524	0.629
F(000)	1034.6	958.5	1917.1	2198.8
Crystal size/mm ³	0.4 × 0.3 × 0.2	0.04 × 0.03 × 0.02	0.04 × 0.03 × 0.02	0.04 × 0.03 × 0.02
Radiation	Mo Kα (λ = 0.71073)			
2 θ range for data collection/°	4.02 to 54.22	4.88 to 55.1	5.86 to 52.84	4.88 to 55.12
Index ranges	-13 ≤ h ≤ 13, -17 ≤ k ≤ 17, -23 ≤ l ≤ 23	-16 ≤ h ≤ 16, -18 ≤ k ≤ 18, -18 ≤ l ≤ 18	-25 ≤ h ≤ 25, -13 ≤ k ≤ 13, -28 ≤ l ≤ 28	-16 ≤ h ≤ 16, -18 ≤ k ≤ 18, -39 ≤ l ≤ 39
Reflections collected	81824	37689	59672	76899
Independent reflections	10344 [R _{int} = 0.0331, R _{sigma} = 0.0189]	10180 [R _{int} = 0.0429, R _{sigma} = 0.0398]	9125 [R _{int} = 0.1108, R _{sigma} = 0.0793]	22825 [R _{int} = 0.0456, R _{sigma} = 0.0564]
Data/restraints/parameters	10344/6/745	10180/132/550	9125/62/550	22825/5/1180
Goodness-of-fit on F ²	1.105	1.037	1.091	1.048
Final R indexes [I≥2σ (I)]	R ₁ = 0.0298, wR ₂ = 0.0735	R ₁ = 0.0472, wR ₂ = 0.1373	R ₁ = 0.0661, wR ₂ = 0.1504	R ₁ = 0.0461, wR ₂ = 0.0963
Final R indexes [all data]	R ₁ = 0.0374, wR ₂ = 0.0829	R ₁ = 0.0702, wR ₂ = 0.1688	R ₁ = 0.1175, wR ₂ = 0.1838	R ₁ = 0.0756, wR ₂ = 0.1098
Largest diff. peak/hole / e Å ⁻³	0.39/-0.59	0.95/-1.11	1.62/-1.18	0.83/-0.76

Table S2 Selected experimental and theoretical bond parameters of **3a** and **3b**.

3a			3b		
	Expt.	Theo.		Expt.	Theo.
Ru1–N1	2.145(2),	2.22749	Ru1–N1	2.160(3)	2.22921
Ru1–N2	2.106(2),	2.13281	Ru1–N2	2.119(3)	2.13152
Ru1–Cl1	2.4323(11)	2.50755	Ru1–Cl1	2.423(9)	2.50952
Ru1–C23	2.001(5)	1.85717	Ru1–C17	1.904(5)	1.85846
Ru1–P1	2.3893(8)	2.47595	Ru1–P1	2.391(8)	2.47388
Ru1–P2	2.3969(8)	2.47450	Ru1–P2	2.408(8)	2.47444
N2–N3	1.351(4)	1.33640	N2–N3	1.356(3)	1.33806
N1–C5	1.357(4)	1.36692	N1–C5	1.350(4)	1.36710
N2–C5	1.341(3)	1.35701	N2–C5	1.348(4)	1.35620
N3–C6	1.285(4)	1.29523	N3–C6	1.286(4)	1.29186
N1–Ru1–N2	61.58(9)	60.75676	N1–Ru1–N2	61.24(10)	60.75003
N1–Ru1–C23	161.53(14)	163.90123	N1–Ru1–C17	165.42(13)	163.94884
N2–Ru1–C23	100.05(16)	103.14454	N2–Ru1–C17	104.19(13)	103.19960
P1–Ru1–P2	177.63(3).	178.90597	P1–Rh1–P2	175.00(11)	178.78847

Table S3 Selected experimental and theoretical bond parameters of **3c** and **4b**.

3c			4b		
	Expt.	Theo.		Expt.	Theo.
Ru1–N1	2.195(4)	2.22877	Ru1–N1	2.217(3)	2.30797
Ru1–N2	2.082(5)	2.13714	Ru1–N2	2.137(3)	2.15018
Ru1–Cl1	2.4527(16)	2.50118	Ru1–Cl1	2.4168(12)	2.49091
Ru1–C17	1.897(7)	1.85562	Ru1–C19	1.930(6),	1.84455
Ru1–P1	2.4032(14)	2.42191	Ru1–P1	2.4032(14)	2.48850
Ru1–P2	2.3864(14)	2.43191	Ru1–P2	2.4069(10)	2.48513
N2–N3	1.349(7)	1.33845	N2–N3	1.361(4)	1.34471
N1–C5	1.361(7)	1.36769	N1–C7	1.324(5)	1.33281
N2–C5	1.355(7)	2.13714	N2–C7	1.338(5)	1.33259
N3–C6	1.281(8)	1.29413	N3–C8	1.297(5)	1.29128
N1–Ru1–N2	61.43(18)	60.67959	N1–Ru1–N2	61.32(13)	60.29950
N1–Ru1–C17	161.9(2)	163.42681	N1–Ru1–C19	163.94(15)	162.40466
N2–Ru1–C17	100.5(2)	102.75808	N2–Ru1–C19	102.62(16)	102.10561
P1–Rh1–P2	177.84(5)	178.85004	P1–Rh1–P2	176.09(3)	179.00815

Absorption Spectra

Time-dependent density functional theory (TD-DFT) analysis in CH_2Cl_2 solvent was carried out using the CPCM model in an effort to elucidate the optical absorption processes. The most pertinent transitions, along with the energies, characters as well as the oscillator strengths of both **3** and **4** are listed in the ESI† (Tables S5, S8, S11, S14 and S17). Natural transition orbital (NTO) analysis was used to inspect the basis of the absorption processes and are portrayed in Tables S6, S9, S12, S15 and S18. This technique offers a compact elucidation of the transition density between the ground and excited states in terms of an expansion into single-particle transitions (hole and electron states for each given excitation). In this case, we refer to the unoccupied and occupied NTOs as “electron” and “hole” transition orbitals, respectively.¹

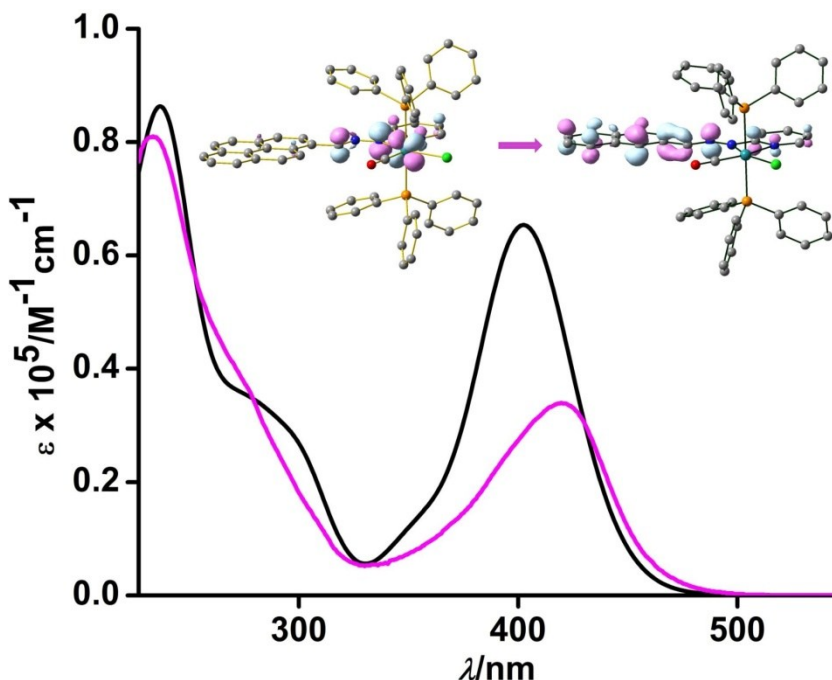


Fig. S1 Experimental (pink) and theoretical (black) absorption spectra of **3b** in dichloromethane.

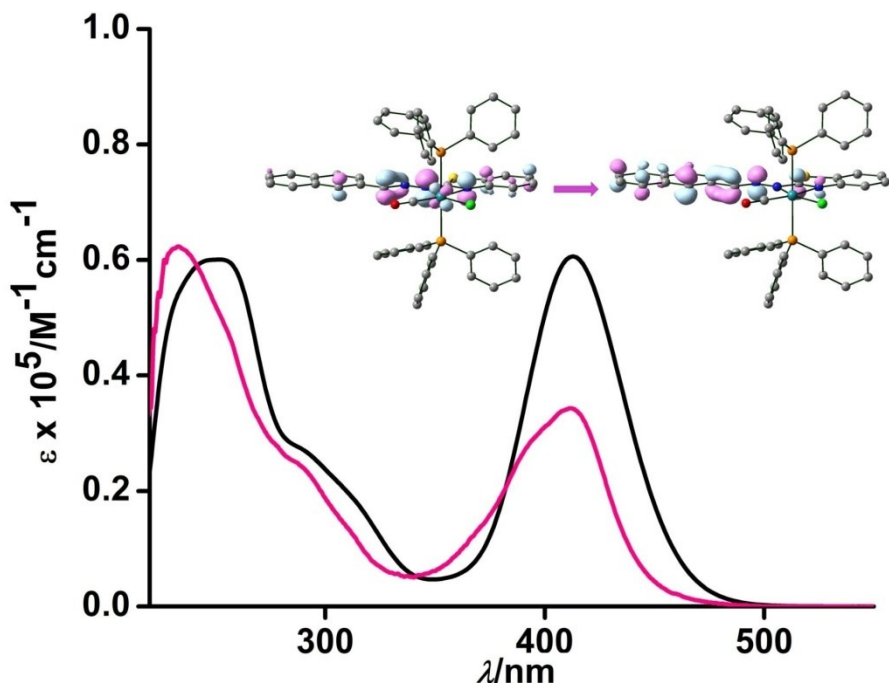


Fig. S2 Experimental (pink) and theoretical (black) absorption spectra of **4b** in dichloromethane.

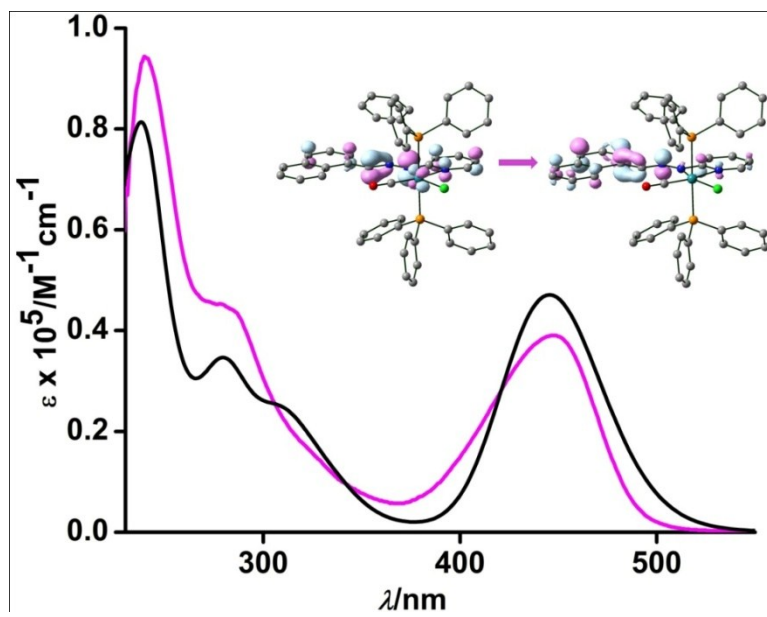


Fig. S3 Experimental (pink) and theoretical (black) absorption spectra of **3c** in dichloromethane.

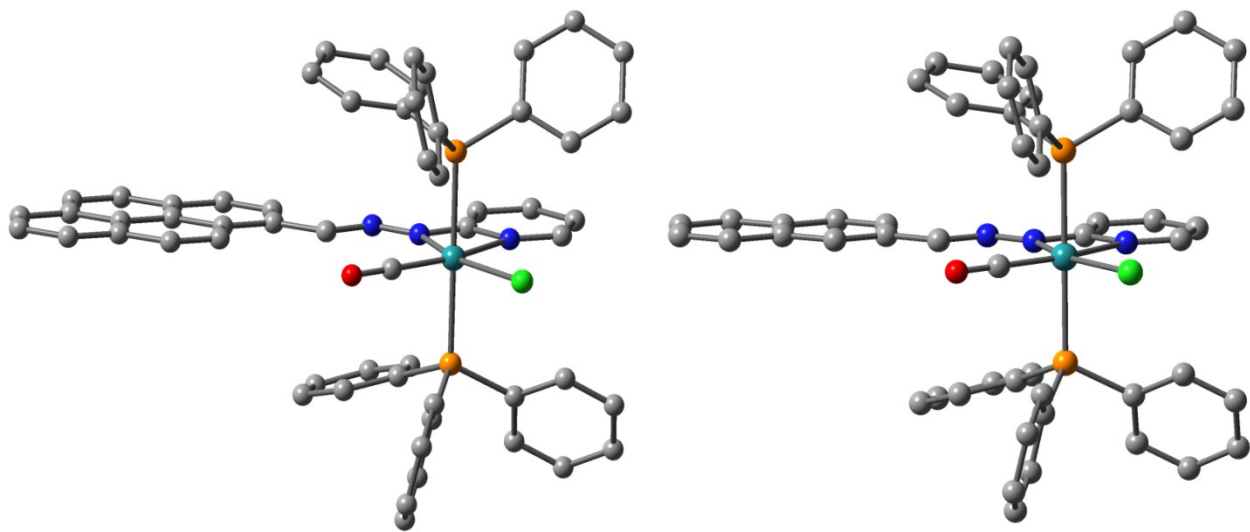


Fig. S4 Optimized geometry of complex **3a**(left) and **3b**(right).

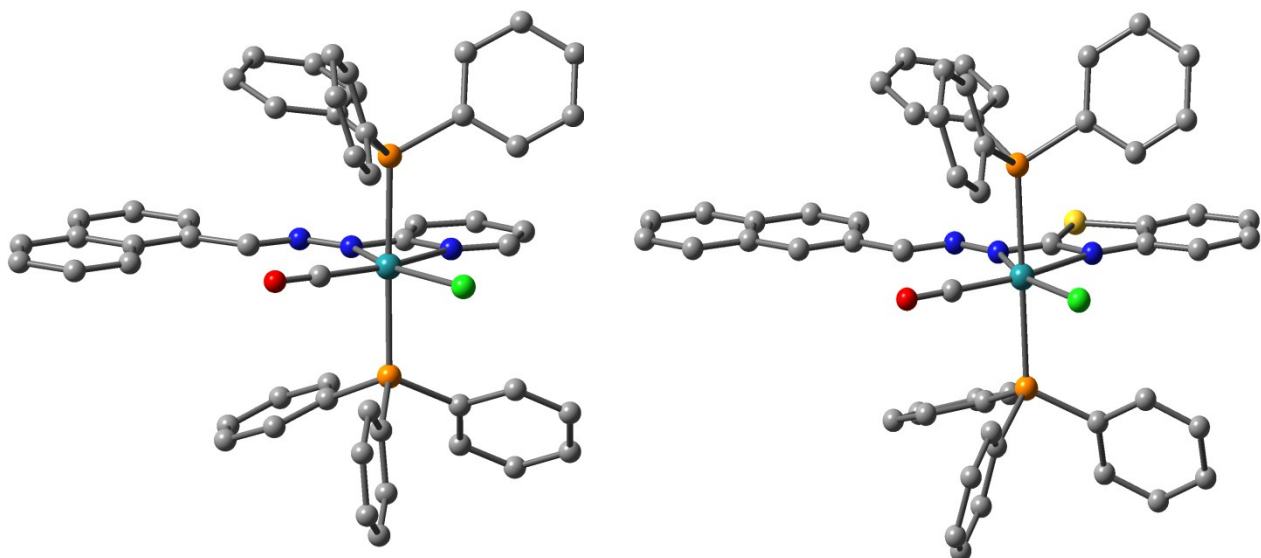


Fig. S5 Optimized geometry of complex **3b**.

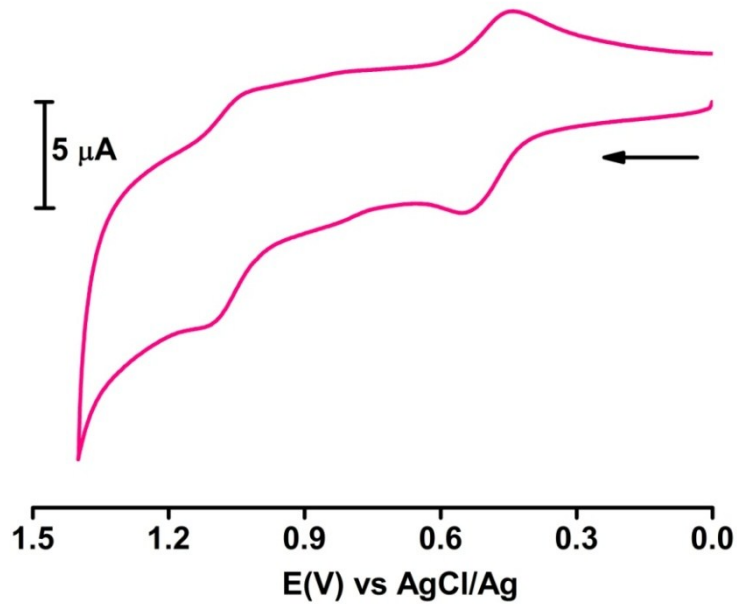


Fig. S6 Cyclic voltammogram of $[Ru^{II}(HL^{Py})(CO)Cl(PPh_3)_2]$ (**3a**) (scan rate:100) in CH_2Cl_2 solvent at 298K. Conditions: 0.20 M $[\text{N}(\text{n}-\text{Bu})_4]\text{PF}_6$ supporting electrolyte; platinum working electrode.

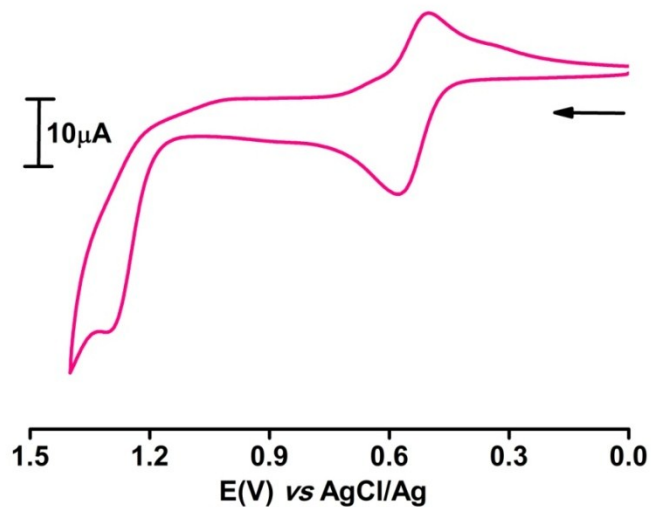


Fig. S7 Cyclic voltammogram of $[Ru^{II}(HL^{Py})(CO)Cl(PPh_3)_2]$ (**3c**) (scan rate:100) in CH_2Cl_2 solvent at 298K. Conditions: 0.20 M $[\text{N}(\text{n}-\text{Bu})_4]\text{PF}_6$ supporting electrolyte; platinum working electrode.

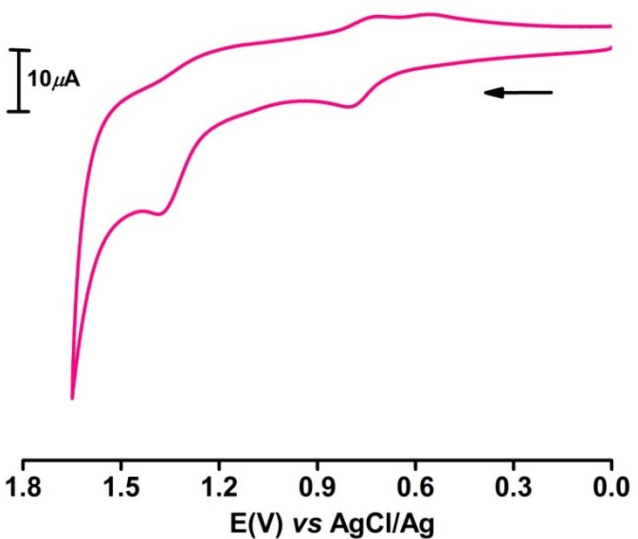


Fig. S8 Cyclic voltammogram of $[Ru^{II}(L^{Benz})(CO)Cl(PPh_3)_2]$ (**4a**) (scan rate:100) in CH_2Cl_2 solvent at 298K. Conditions: 0.20 M $[\text{N}(\text{n-Bu})_4]\text{PF}_6$ supporting electrolyte; platinum working electrode.

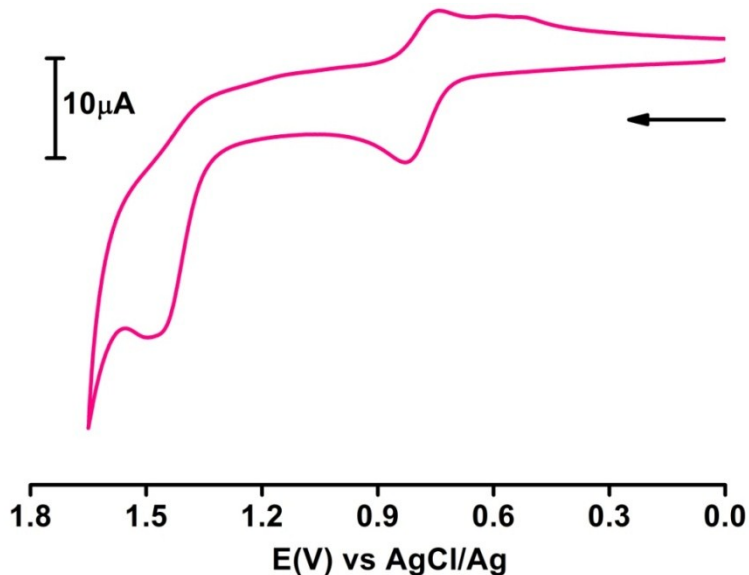


Fig. S9 Cyclic voltammogram of $[Ru^{II}(L^{Benz})(CO)Cl(PPh_3)_2]$ (**4b**) (scan rate:100) in CH_2Cl_2 solvent at 298K. Conditions: 0.20 M $[\text{N}(\text{n-Bu})_4]\text{PF}_6$ supporting electrolyte; platinum working electrode.

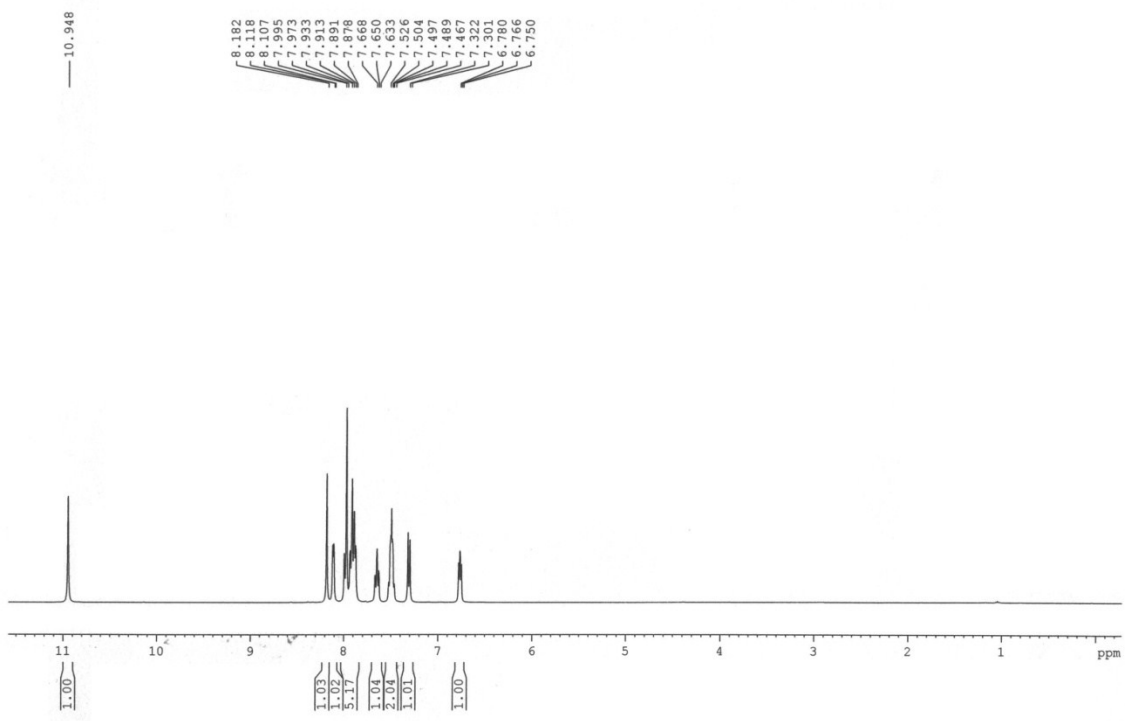


Fig. S10 ^1H -NMR of ligand **1b**.

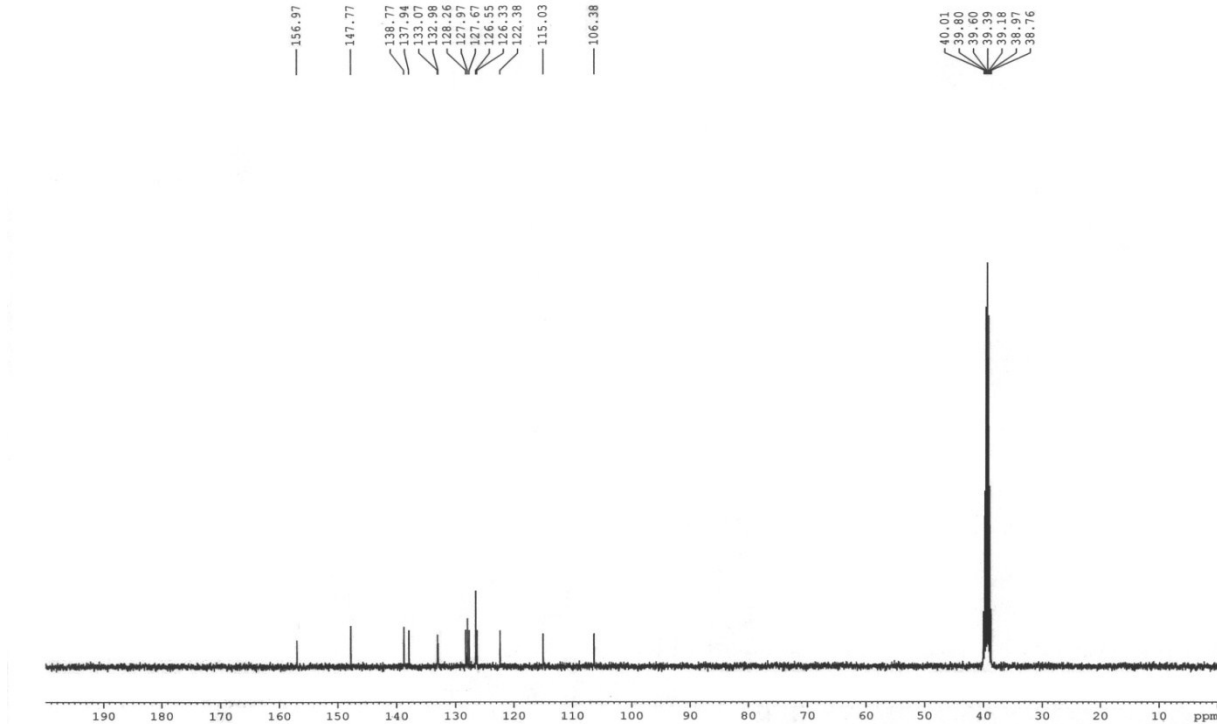


Fig. S11 ^{13}C -NMR of ligand **1b**.

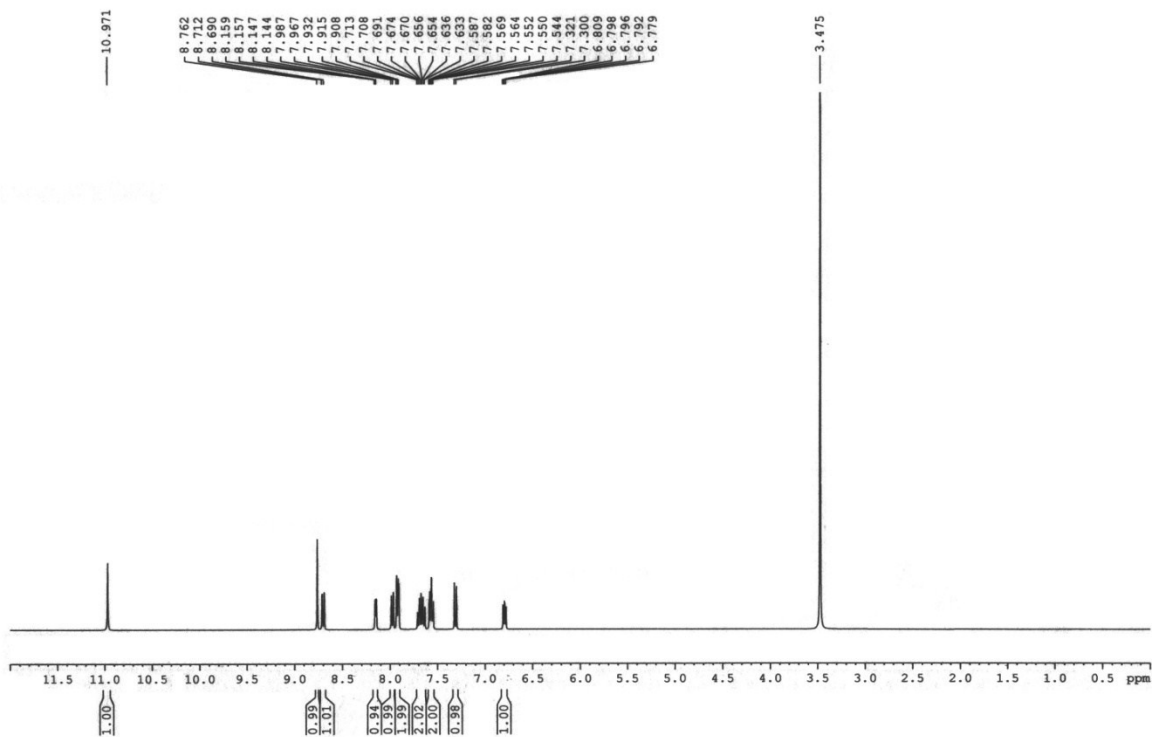


Fig. S12 ^1H -NMR of ligand **1c**.

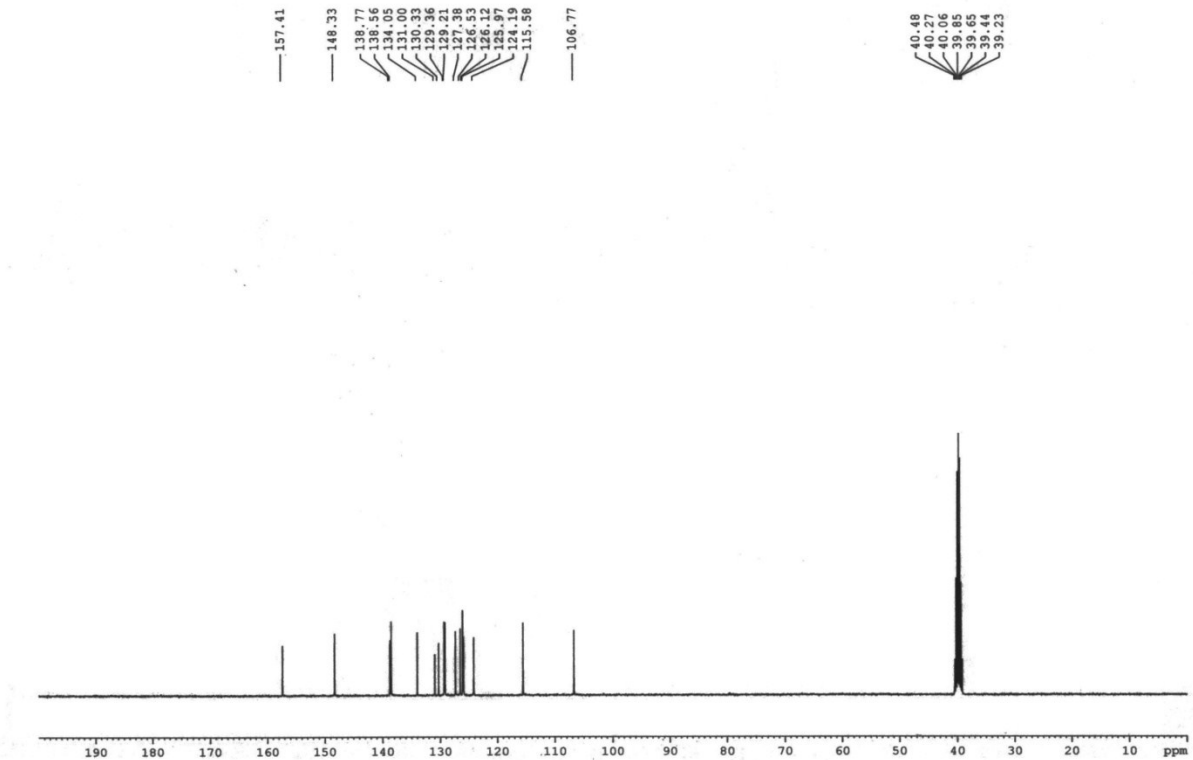


Fig. S13 ^1H -NMR of ligand **2b**.

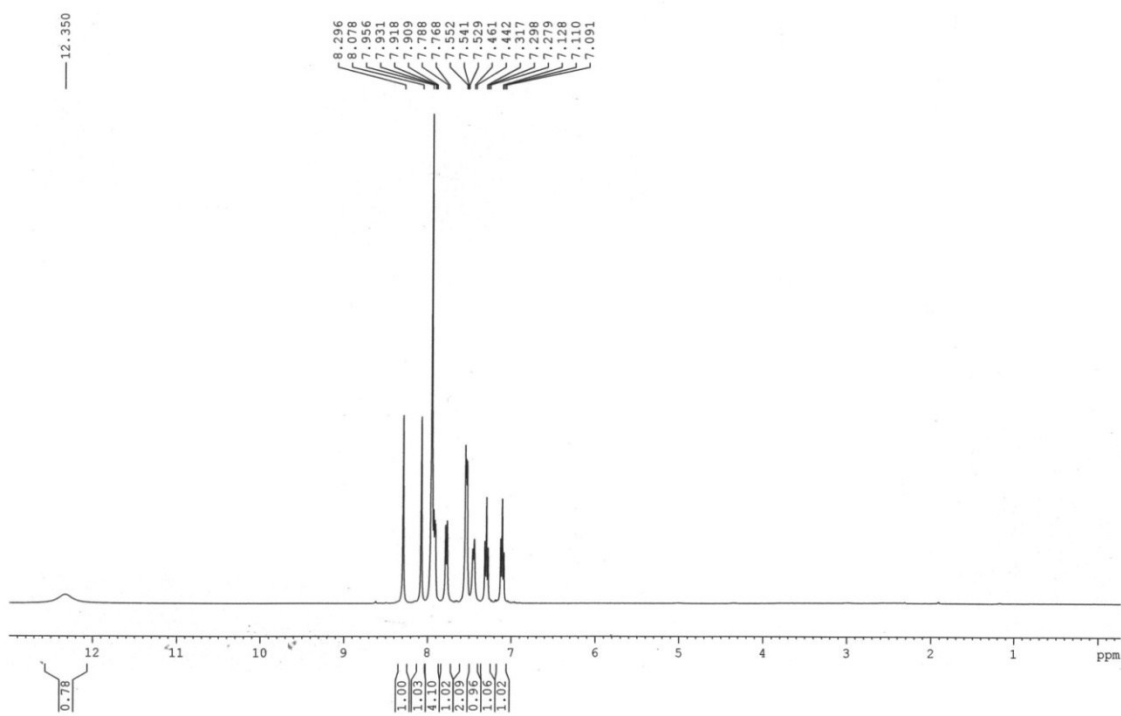


Fig. S14 ^1H -NMR of ligand **2b**.

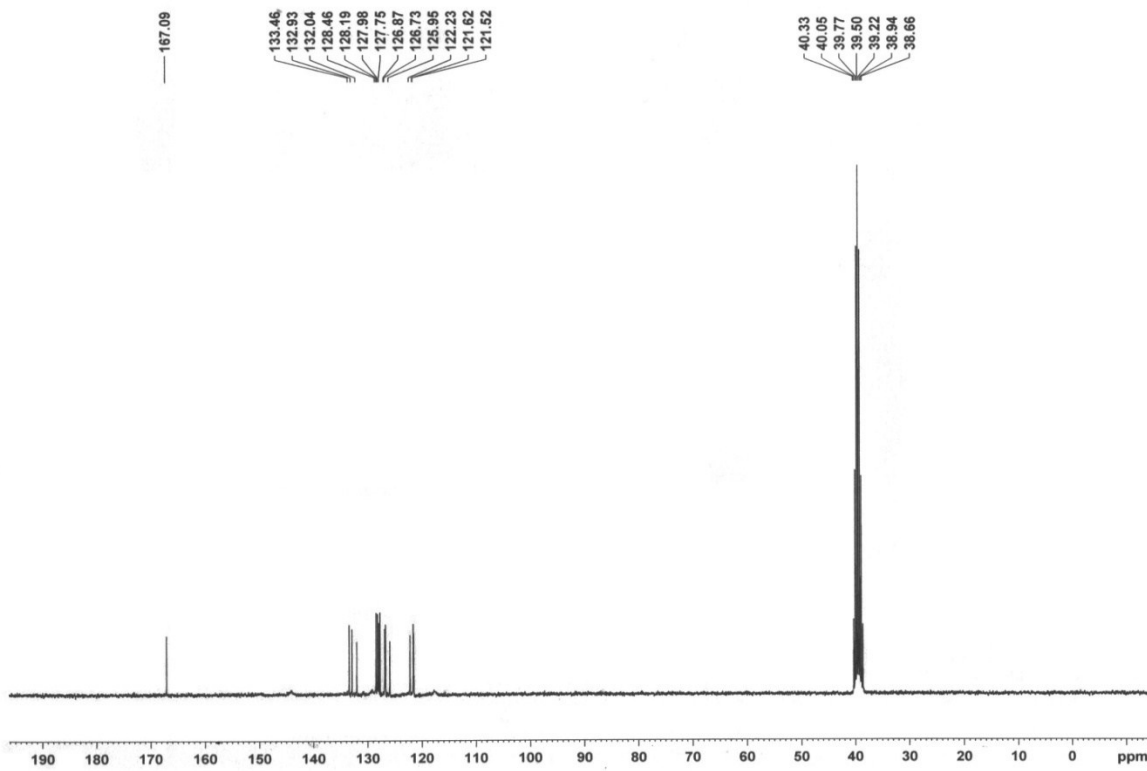


Fig. S15 ^{13}C -NMR of ligand **2b**.

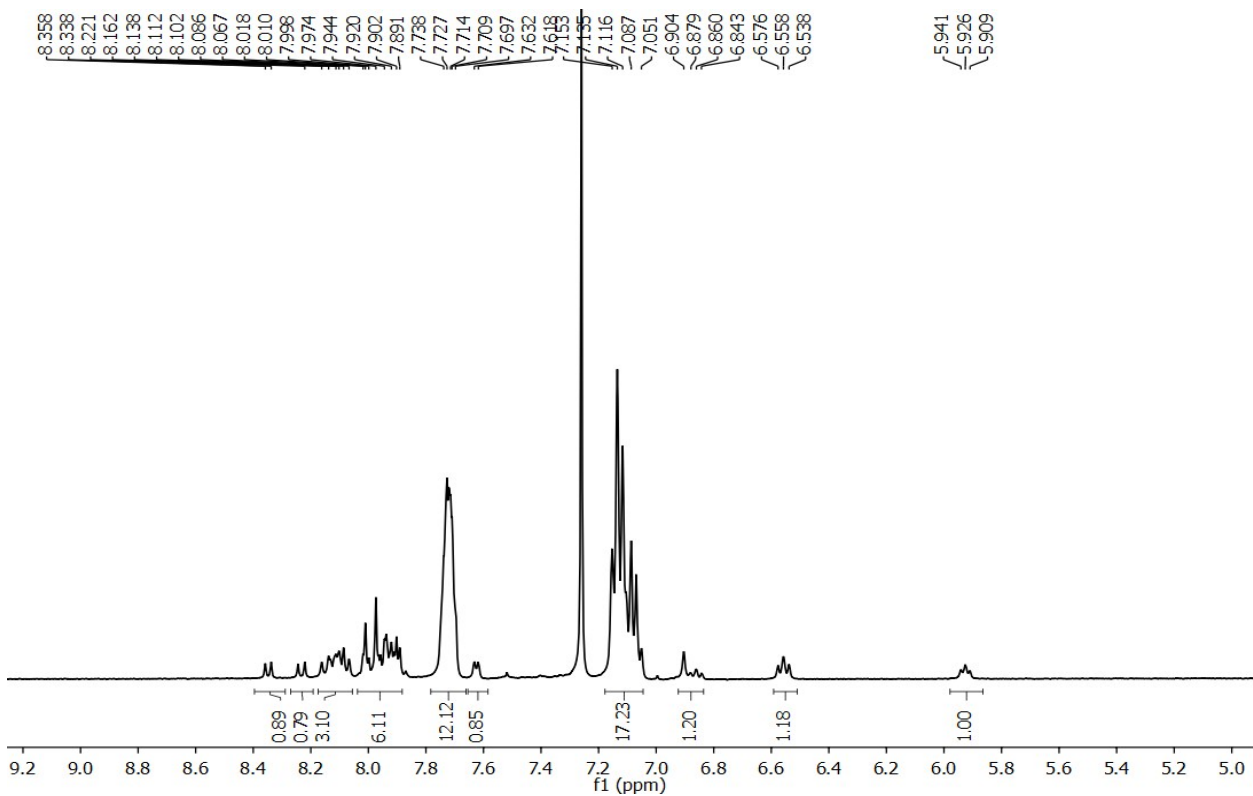


Fig. S16 ^1H -NMR of complex **3a**.

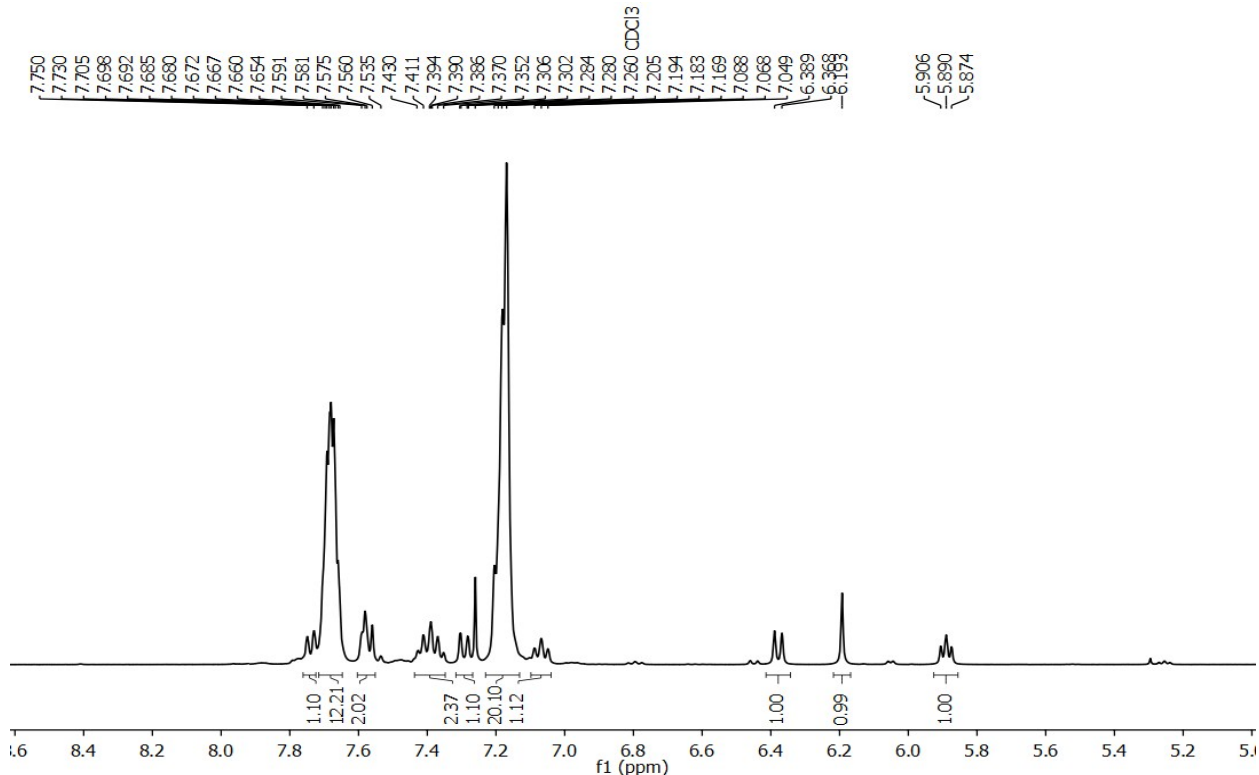


Fig. S17 ^1H -NMR of complex **3b**.

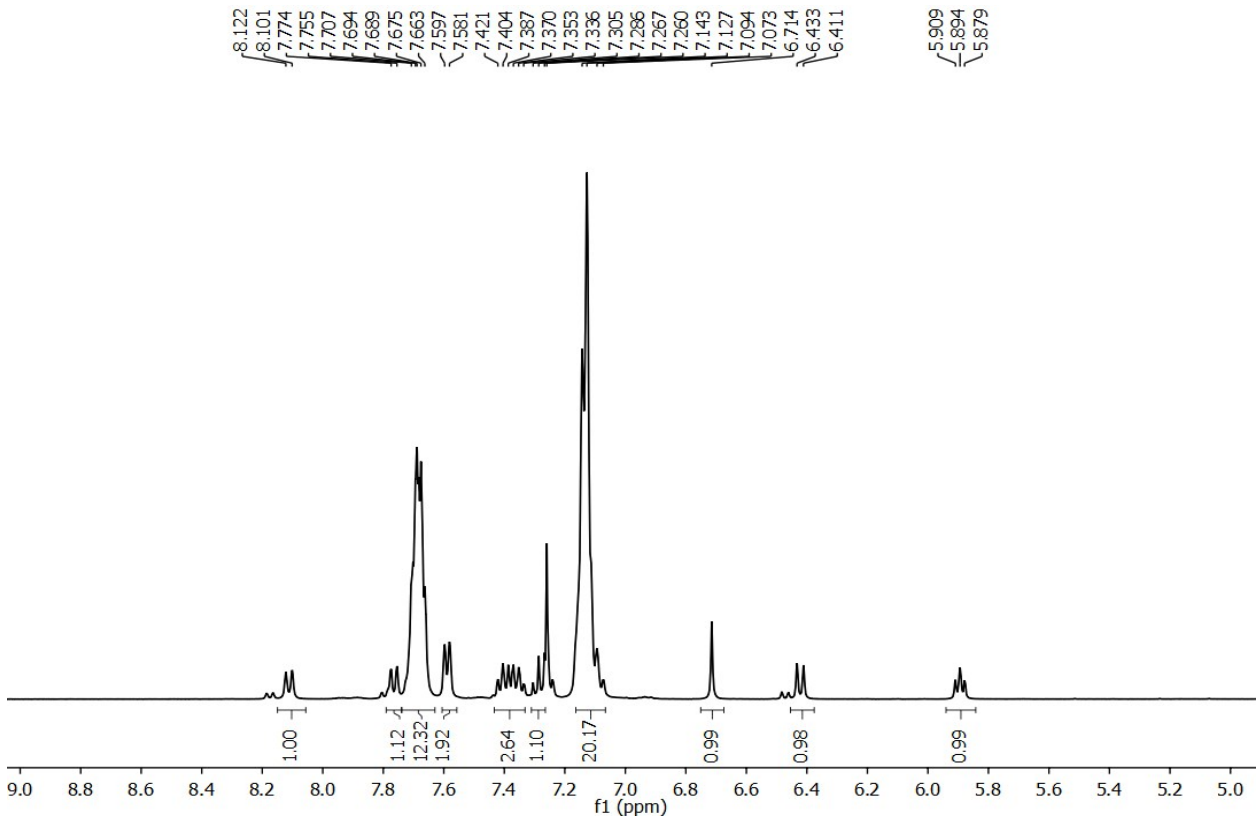


Fig. S18 ^1H -NMR of complex **3c**.

Table S4 Frontier molecular orbital composition (%) in the ground state for **3a**.

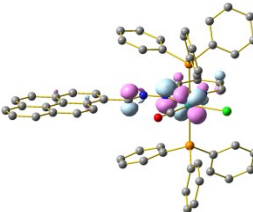
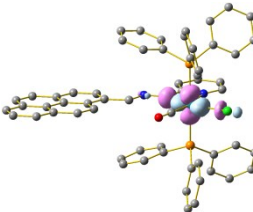
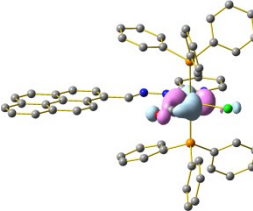
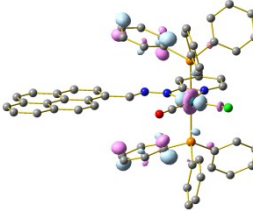
Orbital	MO	Energy (EV)	Contribution (%)							Main Bond Type
			Metal	Ligand						
			Ru	Pyr	Hydrazone	Py	PPh_3	CO	Cl	
251	L+5	-0.65	2	11	2	58	26	2	0	$\pi^*(\text{Py}+\text{Pyr}+\text{PPh}_3)$
250	L+4	-0.72	45	0	6	5	34	4	5	$\text{Ru}+\pi^*(\text{PPh}_3)$
249	L+3	-0.76	3	0	0	0	95	0	1	$\pi^*(\text{PPh}_3)$
248	L+2	-0.82	0	0	0	21	76	3	0	$\pi^*(\text{Py}+\text{PPh}_3)$
247	L+1	-1.13	31	0	4	1	61	1	3	$\text{Ru}+\pi^*(\text{PPh}_3)$
246	LUMO	-1.52	0	77	13	9	0	0	0	$\pi^*(\text{Hydrazone}+\text{Pyr})$
245	HOMO	-4.42	6	38	34	19	1	0	1	$\pi(\text{Hydrazone}+\text{Pyr}+\text{Py})$
244	H-1	-5.38	12	64	11	7	2	0	5	$\pi(\text{Hydrazone}+\text{Pyr}+\text{Py})$
243	H-2	-5.81	21	19	4	4	18	0	34	$\text{Ru}+\pi(\text{Pyr}+\text{Cl}+\text{PPh}_3)$
242	H-3	-5.97	39	0	5	3	3	9	41	$\text{Ru}+\pi(\text{Cl})$
241	H-4	-6.05	2	81	4	7	2	0	4	$\text{Ru}+\pi(\text{Pyr})$
240	H-5	-6.17	24	2	0	8	66	0	0	$\text{Ru}+\pi(\text{PPh}_3)$

HOMO-LUMO gap = 2.90 eV

Table S5 Main optical transition at the TD-DFT/B3LYP/6-31+G(d,p) Level for the complex **3a** with composition in terms of molecular orbital contribution of the transition, Computed Vertical excitation energies, and oscillator strength in dichloromethane.

Transition	CI	Composition	E (eV)	Oscillato r strength (f)	λ_{theo} (nm)
$S_0 \rightarrow S_2$	0.70168	HOMO \rightarrow LUMO (98%)	2.5630	1.0774	483.74
$S_0 \rightarrow S_{12}$	0.36139 0.32129	H-4 \rightarrow L+1 (26%) H-4 \rightarrow L+3 (21%)	3.5887	0.0577	345.49
$S_0 \rightarrow S_{38}$	0.54048	H-1 \rightarrow L+5 (58%)	4.3871	0.0735	282.61

Table S6 Natural transition orbitals (NTOs) for complex **3a** illustrating the nature of singlet excited states in the absorption bands in the range 200–700 nm. For each state, the respective number of the state, transition energy (eV), and the oscillator strength (in parentheses) are listed. Shown are only occupied (holes) and unoccupied (electrons) NTO pairs that contribute more than 10% to each excited state.

		Hole	Electron
483nm	S_2 $w = 0.9847$ $2.5630 (1.0774)$ 483.74 nm LMCT + MMCT $\pi(\text{Hydrazone+Py}) + d_{xy} (\text{Ru}) \rightarrow d_{x^2-y^2}(\text{Ru}) + p(\text{Cl})$		
345 nm	S_{12} $w = 0.2612$ $3.5887 (0.0577)$ 345.49 nm LLCT+MLCT $d_{xz}(\text{Ru}) \rightarrow d_z^2(\text{Ru}) + \pi^*(\text{PPh}_3)$		

S_{12}	w = 0.2064		
	3.5887 (0.0577)		
	345.49 nm		
LLCT+d-d transition	$\pi(\text{CO})+\text{d}_{xz}(\text{Ru}) \rightarrow \text{d}_{xz}(\text{Ru})+\sigma^*(\text{Ru-hydrazone})$		
278 nm	S_{38}	w = 0.5842	
	4.3871 (0.0735)	282.61 nm	
ILCT	$\pi(\text{hydrazone})+\text{d}_{xy}(\text{Ru}) \rightarrow \sigma^*(\text{Ru-P})+\sigma^*(\text{Ru-Cl})$		

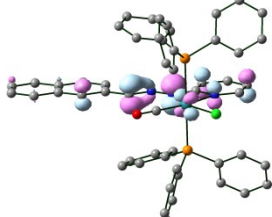
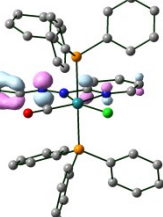
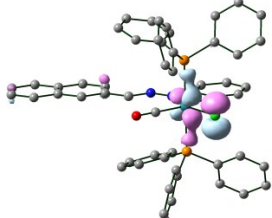
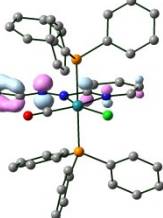
Table S7 Frontier molecular orbital composition (%) in the ground state for **3b**.

Orbital	MO	Energy (EV)	Contribution (%)							Main Bond Type
			Metal		Ligand					
			Ru	Nap	Hydrazone	Py	PPh ₃	CO	Cl	
232	L+5	-0.6	2	10	1	61	24	2	0	$\pi^*(\text{PPh}_3)$
231	L+4	-0.67	44	0	6	5	36	4	5	$\text{Ru} + \pi^*(\text{PPh}_3)$
230	L+3	-0.74	3	0	0	0	96	1	1	$\pi^*(\text{PPh}_3)$
229	L+2	-0.8	0	1	0	16	80	2	0	$\pi^*(\text{Py}+\text{PPh}_3)$
228	L+1	-1.07	0	61	20	17	2	0	0	$\pi^*(\text{Nap}+\text{Hydrazone}+\text{PPh}_3)$
227	LUMO	-1.1	30	1	4	1	62	1	2	$\text{Ru} + \pi^*(\text{Pyr}+\text{Hydrazone})$
226	HOMO	-4.53	9	21	42	25	1	0	1	$\pi(\text{Nap}+\text{Hydrazone}+\text{Py})$
225	H-1	-5.65	18	56	2	0	6	0	17	$\text{Ru} + \pi(\text{Naph}+\text{Cl})$
224	H-2	-5.8	13	40	4	4	14	0	24	$\text{Ru} + \pi(\text{Nap}+\text{PPh}_3+\text{Cl})$
223	H-3	-5.93	40	0	5	3	3	9	40	$\text{Ru} + \pi(\text{Cl})$
222	H-4	-6.14	24	0	1	11	63	0	0	$\text{Ru} + \pi(\text{Py}+\text{PPh}_3)$
221	H-5	-6.39	1	69	6	13	8	0	2	$\pi(\text{Nap}+\text{Py})$
HOMO-LUMO gap = 3.43 eV										

Table S8 Main optical transition at the TD-DFT/B3LYP/6-31+G(d,p) Level for the complex **3b** with composition in terms of molecular orbital contribution of the transition, Computed Vertical excitation energies, and oscillator strength in dichloromethane.

Transition	CI	Composition	E (eV)	Oscillator strength (<i>f</i>)	λ_{theo} (nm)
$S_0 \rightarrow S_3$	0.67377	HOMO \rightarrow L+1 (91%)	3.077 4	0.8706	402.88
$S_0 \rightarrow S_{25}$	0.59685	H-2 \rightarrow L+1 (71%)	4.308 1	0.0764	287.79
$S_0 \rightarrow S_{97}$	0.38806	H-5 \rightarrow L+2 (30%)	5.274 2	0.0397	235.08

Table S9 Natural transition orbitals (NTOs) for complex **3b** illustrating the nature of singlet excited states in the absorption bands in the range 200–700 nm. For each state, the respective number of the state, transition energy (eV), and the oscillator strength (in parentheses) are listed. Shown are only occupied (holes) and unoccupied (electrons) NTO pairs that contribute more than 10% to each excited state.

		Hole	Electron
419 nm	S_3 w = 0.9079 3.0774 (0.8706) 402.88 nm		
272 nm	ILCT+MLCT $\pi(\text{Hydrazone+Nap}) + d_{yz}(\text{Ru}) \rightarrow \pi^*(\text{Hydrazone+Nap})$		
	S_{25} w = 0.7118 4.3081 (0.0764) 287.79 nm		
	LLCT $\sigma(\text{Ru-P}) + p(\text{Cl}) \rightarrow \pi^*(\text{Hydrazone+Nap})$		

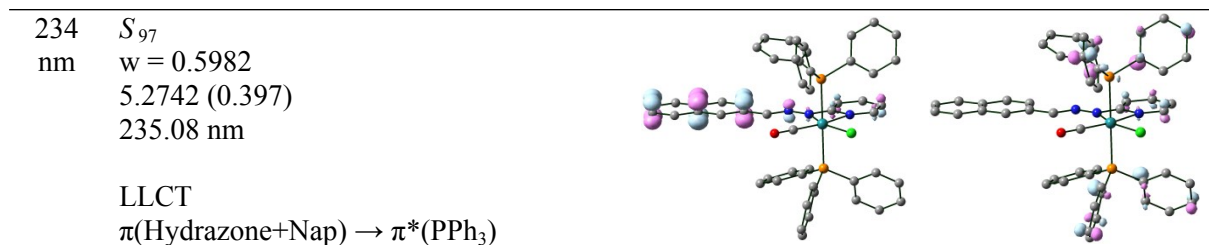


Table S10 Frontier molecular orbital composition (%) in the ground state for **3c**.

Orbital	MO	Energy (eV)	Contribution (%)							Main Bond Type
			Metal	Ligand						
			Ru	Nap	Hydrazone	Py	PPh ₃	CO	Cl	
232	L+5	-0.95	1	0	2	53	42	1	0	$\pi^*(\text{PPh}_3)$
231	L+4	-1.02	31	0	3	0	39	28	3	$\text{Ru} + \pi^*(\text{PPh}_3)$
230	L+3	-1.06	2	1	0	23	74	0	0	$\pi^*(\text{PPh}_3)$
229	L+2	-1.17	2	0	0	14	81	4	0	$\pi^*(\text{Py}+\text{PPh}_3)$
228	L+1	-1.41	28	5	4	1	60	0	2	$\pi^*(\text{Nap}+\text{Hydrazone}+\text{PPh}_3)$
227	LUMO	-1.55	2	59	19	14	6	0	0	$\text{Ru} + \pi^*(\text{Pyr}+\text{Hydrazone})$
226	HOMO	-4.77	8	26	40	24	0	0	1	$\pi(\text{Nap}+\text{Hydrazone}+\text{Py})$
225	H-1	-5.9	28	38	3	1	7	0	23	$\text{Ru} + \pi(\text{Naph}+\text{Cl})$
224	H-2	-6.17	28	9	13	1	5	8	36	$\text{Ru} + \pi(\text{Nap}+\text{PPh}_3+\text{Cl})$
223	H-3	-6.18	14	28	11	9	11	3	24	$\text{Ru} + \pi(\text{Cl})$
222	H-4	-6.39	23	0	1	10	66	0	0	$\text{Ru} + \pi(\text{Py}+\text{PPh}_3)$
221	H-5	-6.61	0	99	0	0	1	0	0	$\pi(\text{Nap}+\text{Py})$
HOMO–LUMO gap = 3.22 eV										

Table S11 Main optical transition at the TD-DFT/B3LYP/6-31+G(d,p) Level for the complex **3c** with composition in terms of molecular orbital contribution of the transition, Computed Vertical excitation energies, and oscillator strength in dichloromethane.

Transition	CI	Composition	E (eV)	Oscillator strength (f)	λ_{theo} (nm)
$S_0 \rightarrow S_2$	0.68705	HOMO \rightarrow LUMO (94%)	2.7858	0.6432	445.05

$S_0 \rightarrow S_{37}$	0.54935	H-5 → LUMO (60%)	4.4773	0.1077	276.92
$S_0 \rightarrow S_{112}$	0.24533	H-7 → L+3 (22%)	5.2151	0.0970	237.74

Table S12 Natural transition orbitals (NTOs) for complex **3c** illustrating the nature of singlet excited states in the absorption bands in the range 200–700 nm. For each state, the respective number of the state, transition energy (eV), and the oscillator strength (in parentheses) are listed. Shown are only occupied (holes) and unoccupied (electrons) NTO pairs that contribute more than 10% to each excited state.

		Hole	Electron
419	S_2		
nm	w = 0.9440 2.7858 (0.6432) 445.05 nm		
	ILCT+MLCT $\pi(\text{Hydrazone+Nap+Py}) + d_{yz}(\text{Ru}) \rightarrow \pi^*(\text{Hydrazone+Nap})$		
272	S_{37}		
nm	w = 0.6035 4.4773 (0.1077) 276.92 nm		
	ILCT $\pi^*(\text{Nap}) \rightarrow \pi^*(\text{Hydrazone+Nap})$		
234	S_{112}		
nm	w = 0.1203 5.2151 (0.0970) 237.74 nm		
	LLCT $\pi(\text{PPh}_3) \rightarrow \sigma^*(\text{Ru-N}_{\text{hydrazone}}) + \sigma^*(\text{Ru-N}_{\text{Py}})$		

Table S13 Frontier molecular orbital composition (%) in the ground state for **4a**.

Orbital	MO	Energy (EV)	Contribution (%)							Main Bond Type
			Metal	Ligand						
			Ru	Pyr	Hydrazone	Benz	PPh ₃	CO	Cl	
265	L+5	-0.93	6	1	2	0	85	7	1	$\pi^*(\text{PPh}_3)$
264	L+4	-1.12	1	72	17	9	0	1	0	$\pi^*(\text{Pyr}+\text{Hydrazone})$
263	L+3	-1.14	5	1	2	0	87	5	1	$\pi^*(\text{PPh}_3)$
262	L+2	-1.2	32	3	0	0	31	32	4	$\text{Ru}+\pi^*(\text{PPh}_3+\text{CO})$
261	L+1	-1.57	32	1	0	1	61	2	2	$\text{Ru}+\pi^*(\text{PPh}_3)$
260	LUMO	-2.05	0	72	16	11	0	0	0	$\pi^*(\text{Pyr}+\text{Hydrazone}+\text{Benz})$
259	HOMO	-4.91	6	37	29	27	0	0	1	$\pi(\text{Pyr}+\text{Hydrazone}+\text{Benz})$
258	H-1	-5.77	10	62	9	13	1	0	5	$\text{Ru}+\pi(\text{Pyr}+\text{Benz})$
257	H-2	-6.07	35	4	2	23	5	0	32	$\text{Ru}+\pi(\text{Benz}+\text{Cl})$
256	H-3	-6.27	16	6	2	18	35	2	19	$\text{Ru}+\pi(\text{Benz}+\text{PPh}_3+\text{Cl})$
255	H-4	-6.29	26	3	2	17	11	7	34	$\text{Ru}+\pi(\text{Benz}+\text{PPh}_3+\text{Cl})$
254	H-5	-6.43	0	80	1	16	2	0	0	$\pi(\text{Pyr}+\text{Benz})$
HOMO-LUMO gap = 2.86 eV										

Table S14 Main optical transition at the TD-DFT/B3LYP/6-31+G(d,p) Level for the complex **4a** with composition in terms of molecular orbital contribution of the transition, Computed Vertical excitation energies, and oscillator strength in dichloromethane.

Transition	CI	Composition	E (eV)	Oscillator strength (f)	λ_{theo} (nm)
$S_0 \rightarrow S_2$	0.69064	HOMO \rightarrow LUMO (95%)	2.5373	1.2314	488.64
$S_0 \rightarrow S_7$	0.50542	H-1 \rightarrow LUMO (51%)	3.4794	0.0701	356.34
$S_0 \rightarrow S_{35}$	0.48982	H-1 \rightarrow L+4 (48%)	4.2506	0.1068	291.69
$S_0 \rightarrow S_{144}$	0.37762	H-4 \rightarrow L+6 (29%)	5.2285	0.0367	237.13

Table S15 Natural transition orbitals (NTOs) for complex **4a** illustrating the nature of singlet excited states in the absorption bands in the range 200–700 nm. For each state, the respective number of the state,

transition energy (eV), and the oscillator strength (in parentheses) are listed. Shown are only occupied (holes) and unoccupied (electrons) NTO pairs that contribute more than 10% to each excited state.

		Hole	Electron
470	S_2 nm w = 0.9539 2.5373 (1.2314) 488.64 nm		
	ILCT+MLCT $\pi(\text{Hydrazone}+\text{Pyr})+\text{d}_{xz}(\text{Ru}) \rightarrow \pi^*(\text{Pyr})$		
350	S_7 nm w = 0.5108 3.4794 (0.0701) 356.34 nm		
	ILCT+MLCT $\pi(\text{Hydrazone}+\text{Pyr})+\text{d}_{xz}(\text{Ru}) \rightarrow \pi^*(\text{Pyr})$		
280	S_{35} nm w = 0.4798 4.2506 (0.1068) 291.69 nm		
	ILCT+LMCT $\pi(\text{Hydrazone}+\text{Pyr})+\text{d}_{xz}(\text{Ru}) \rightarrow \pi^*(\text{Pyr})$		
231	S_{144} nm w = 0.2851 5.2285 (0.0367) 237.13 nm		
	LLCT $\pi(\text{Pyr}) \rightarrow \pi^*(\text{PPh}_3)$		

Table S16 Frontier molecular orbital composition (%) in the ground state for **4b**.

Orbital	MO	Energy (EV)	Contribution (%)							Main Bond Type
			Metal		Ligand					
			Ru	Nap	Hydrazone	Benz	PPh ₃	CO	Cl	
246	L+5	-1.05	0	78	8	6	8	0	0	$\pi^*(\text{Nap})$
245	L+4	-1.14	17	1	3	0	69	8	3	$\text{Ru}+(\text{PPh}_3)$
244	L+3	-1.16	0	0	0	1	95	3	0	$\pi^*(\text{PPh}_3)$
243	L+2	-1.2	26	2	0	0	45	28	3	$\text{Ru}+\pi^*(\text{PPh}_3+\text{CO})$
242	L+1	-1.52	34	0	2	0	61	0	3	$\text{Ru}+\pi^*(\text{PPh}_3)$
241	LUMO	-1.62	0	58	24	18	0	0	0	$\pi^*(\text{Nap}+\text{Hydrazone}+\text{Benz})$
240	HOMO	-5.01	8	18	36	36	0	0	1	$\pi(\text{Nap}+\text{Hydrazone}+\text{Benz})$
239	H-1	-6.03	33	22	2	2	10	0	31	$\text{Ru}+\pi(\text{Nap}+\text{Cl})$
238	H-2	-6.11	9	57	2	25	1	0	5	$\pi(\text{Nap}+\text{Benz})$
237	H-3	-6.24	6	14	2	41	33	0	4	$\pi(\text{Nap}+\text{Benz}+\text{PPh}_3)$
236	H-4	-6.34	37	0	7	0	3	11	45	$\text{Ru}+\pi(\text{CO}+\text{Cl})$
235	H-5	-6.51	6	7	1	59	27	0	0	$\pi(\text{Benz}+\text{PPh}_3)$
HOMO-LUMO gap = 3.39 eV										

Table S17 Main optical transition at the TD-DFT/B3LYP/6-31+G(d,p) Level for the complex **4b** with composition in terms of molecular orbital contribution of the transition, Computed Vertical excitation energies, and oscillator strength in dichloromethane.

Transition	CI	Composition	E (eV)	Oscillat or strength (f)	λ_{theo} (nm)
$S_0 \rightarrow S_3$	0.70062	HOMO \rightarrow LUMO (98%)	3.0077	1.0856	412.23
$S_0 \rightarrow S_{27}$	0.34072	H-4 \rightarrow L+1 (23%)	4.2812	0.1406	289.60
$S_0 \rightarrow S_{63}$	0.43379	H-3 \rightarrow L+5 (38%)	4.8322	0.1061	256.58

Table S18 Natural transition orbitals (NTOs) for complex **4b** illustrating the nature of singlet excited states in the absorption bands in the range 200–700 nm. For each state, the respective number of the state, transition energy (eV), and the oscillator strength (in parentheses) are listed. Shown are only occupied (holes) and unoccupied (electrons) NTO pairs that contribute more than 10% to each excited state.

		Hole	Electron
410	S_3		
nm	w = 0.817 3.0077 (1.0856) 412.23 nm		
	ILCT+MLCT $\pi(\text{Hydrazone}+\text{Benz})+\text{d}_{xz}(\text{Ru}) \rightarrow \pi^*(\text{Nap}+\text{Hydrazone})$		
289	S_{27}		
nm	w = 0.2321 4.2812 (0.1406) 289.60 nm		
	LMCT+d-d transition $\pi(\text{Benz})+\text{d}_{yz}(\text{Ru})+\text{p}(\text{Cl}) \rightarrow \text{d}_{x^2-y^2}(\text{Ru})$		
232	S_{63}		
nm	w = 0.3763 4.8322 (0.1061) 256.58 nm		
	ILCT+LLCT $\pi(\text{Benz}+\text{PPh}_3)+\text{p}(\text{Cl}) \rightarrow \pi^*(\text{Nap})$		

Table S19 Coordinates of optimized geometry of complex **3a**.

Tag	Symbol	X	Y	Z
1	Ru	-1.60877	11.454	4.688899
2	P	-0.97052	13.60587	5.730673
3	P	-2.22385	9.277964	3.680511
4	Cl	-3.6849	12.50202	3.751267
5	N	-2.37644	10.74132	6.654724
6	N	-0.28673	10.43441	6.016125
7	N	0.965056	9.991504	6.16716
8	C	-1.1705	10.21265	7.021741
9	C	-2.4944	9.230421	1.847444
10	C	0.680284	13.47428	6.545567
11	C	-3.47606	14.09702	6.907208
12	C	-3.42634	10.64963	7.479474
13	C	-0.5564	17.33518	2.961176
14	C	-0.77864	15.07139	4.612252

15	C	2.058281	12.7668	8.419888
16	C	-0.88538	8.033521	3.939005
17	C	-1.2271	16.19994	2.509567
18	C	-3.76514	8.459716	4.303879
19	C	-0.9979	9.566294	8.266162
20	C	-2.71016	10.40803	1.119719
21	C	0.147185	7.902674	2.996048
22	C	-2.54433	7.996532	1.174278
23	C	-2.49674	15.62103	9.03145
24	C	-1.61176	15.05798	8.111101
25	C	-4.35746	14.66826	7.827276
26	C	1.817444	10.20736	5.216121
27	C	-0.00276	17.347	4.244547
28	C	-3.87221	15.42651	8.893383
29	C	3.194971	9.741114	5.310514
30	C	3.596329	8.983051	6.430299
31	C	-3.33746	10.02878	8.718854
32	C	1.85102	13.75391	5.822097
33	C	-0.11595	16.22651	5.064875
34	C	-4.86799	9.26653	4.625985
35	C	4.887923	8.510732	6.567403
36	C	-5.11463	6.489011	4.760145
37	C	-2.98562	9.126642	-0.91749
38	C	-3.90478	7.063313	4.367409
39	C	6.135913	10.56993	2.280675
40	C	-2.95272	10.35293	-0.25596
41	C	6.478189	9.803993	3.43613
42	C	-2.78361	7.94583	-0.1972
43	C	5.494381	9.53409	4.43874
44	C	5.863546	8.768313	5.586278
45	C	-0.8018	7.300065	5.133369
46	C	1.220315	7.041676	3.230413
47	C	-6.2044	7.298575	5.084835
48	C	-2.0979	9.484543	9.103805
49	C	3.215158	13.06422	7.697947
50	C	7.115498	10.82529	1.306736
51	C	-6.07794	8.686369	5.011403
52	C	7.813366	9.310164	3.581087
53	C	7.207649	8.285713	5.705687
54	C	4.154497	10.02608	4.295157
55	C	1.283608	6.303779	4.412888
56	C	4.790611	11.05182	2.162519
57	C	8.7599	9.590316	2.580277
58	C	0.271025	6.438602	5.364098
59	C	8.41314	10.33907	1.457524
60	C	3.107543	13.55481	6.396218
61	C	3.851393	10.79479	3.116184
62	C	8.142965	8.542714	4.748094
63	C	-0.52905	11.83354	3.226284

64	O	0.183484	12.05074	2.333243
65	C	-2.0913	14.2822	7.042558
66	C	0.80103	12.96459	7.848464
67	C	-1.34083	15.07309	3.328823
68	H	-4.78333	10.34613	4.55211
69	H	-6.92382	9.325186	5.251843
70	H	-3.11945	11.27559	-0.80511
71	H	-2.723	11.36352	1.629937
72	H	-7.14656	6.849591	5.388236
73	H	-5.20358	5.406792	4.808126
74	H	-3.0706	6.416626	4.116994
75	H	0.112846	8.467526	2.069705
76	H	2.008992	6.953872	2.488382
77	H	2.121072	5.6364	4.595869
78	H	0.315677	5.87636	6.293008
79	H	-1.57235	7.400191	5.891002
80	H	-2.38782	7.071276	1.719923
81	H	-2.81345	6.98445	-0.70321
82	H	-3.1724	9.086732	-1.98745
83	H	-3.86123	13.52628	6.068353
84	H	-5.42726	14.52004	7.704971
85	H	-4.56026	15.86745	9.609981
86	H	-2.1082	16.21454	9.854966
87	H	-0.54655	15.22118	8.234897
88	H	0.321797	16.25094	6.057859
89	H	0.517264	18.22945	4.607927
90	H	-0.46773	18.20946	2.321609
91	H	-1.6703	16.18456	1.517584
92	H	-1.89575	14.21016	2.981376
93	H	1.786078	14.13711	4.808453
94	H	4.001229	13.77767	5.820042
95	H	4.193624	12.90614	8.142818
96	H	2.130809	12.37471	9.430813
97	H	-0.08608	12.71704	8.422786
98	H	-4.35224	11.08866	7.122935
99	H	-4.20622	9.970456	9.364806
100	H	-2.00093	8.993907	10.06937
101	H	-0.02896	9.160264	8.526845
102	H	2.852541	8.772252	7.190602
103	H	5.162484	7.927189	7.443577
104	H	7.468023	7.703627	6.586906
105	H	9.158919	8.169562	4.853308
106	H	9.773664	9.213498	2.693388
107	H	9.159295	10.54546	0.694726
108	H	6.848582	11.40934	0.429214
109	H	4.525734	11.636	1.28429
110	H	2.851233	11.18589	2.970333
111	H	1.494921	10.74547	4.327443

Table S20 Coordinates of optimized geometry of complex **3b**.

Tag	Symbol	X	Y	Z
1	Ru	-1.62214	11.42201	4.660853
2	P	-0.93967	13.57279	5.676352
3	P	-2.28742	9.24679	3.6883
4	Cl	-3.692	12.49928	3.737343
5	N	-2.36835	10.73836	6.647094
6	N	-0.29476	10.39513	5.975003
7	N	0.953795	9.933415	6.11042
8	C	-1.16372	10.19473	6.996778
9	C	-2.57724	9.17872	1.85861
10	C	0.717292	13.42669	6.477252
11	C	-3.42518	14.10866	6.877419
12	C	-3.40427	10.66892	7.491816
13	C	-0.5013	17.27633	2.875756
14	C	-0.73965	15.02826	4.546057
15	C	2.102147	12.70792	8.34244
16	C	-0.97351	7.977277	3.953183
17	C	-1.18443	16.14399	2.435743
18	C	-3.83877	8.467721	4.337014
19	C	-0.97869	9.555486	8.243561
20	C	-2.79409	10.34989	1.120727
21	C	0.050741	7.813395	3.006476
22	C	-2.64454	7.938025	1.199717
23	C	-2.40003	15.62951	8.982134
24	C	-1.53378	15.04864	8.055059
25	C	-4.28776	14.69761	7.804133
26	C	1.798928	10.12418	5.15216
27	C	0.056553	17.29342	4.157271
28	C	-3.77964	15.45443	8.860565
29	C	3.171118	9.639206	5.233869
30	C	3.641948	8.912405	6.371159
31	C	-3.30255	10.05689	8.734362
32	C	1.885275	13.69505	5.745309
33	C	-0.06474	16.18081	4.987072
34	C	-4.91765	9.300746	4.672998
35	C	4.934892	8.460663	6.431394
36	C	-5.22589	6.530044	4.821127
37	C	-3.10528	9.04825	-0.89849
38	C	-4.0094	7.075093	4.407995
39	C	-3.05501	10.28143	-0.25095
40	C	6.304069	9.664658	3.155263
41	C	-2.90208	7.874006	-0.16794
42	C	5.393707	9.425004	4.22092
43	C	5.853079	8.697271	5.36763
44	C	-0.89912	7.256156	5.155626
45	C	1.105727	6.93142	3.244946
46	C	-6.29184	7.365574	5.159031

47	C	-2.06432	9.496859	9.101271
48	C	3.256569	12.9948	7.612354
49	C	-6.13473	8.749793	5.078596
50	C	7.602888	9.208593	3.217891
51	C	7.195426	8.241319	5.401315
52	C	4.050723	9.879462	4.188041
53	C	1.159981	6.206355	4.435773
54	C	0.156375	6.37474	5.391058
55	C	3.143868	13.48544	6.311132
56	C	8.054438	8.489679	4.351237
57	C	-0.5627	11.76956	3.174011
58	O	0.130755	11.96617	2.262595
59	C	-2.03641	14.27429	6.996084
60	C	0.842843	12.91703	7.779754
61	C	-1.3062	15.02499	3.264605
62	H	-4.80915	10.37785	4.594105
63	H	-6.96197	9.408684	5.329521
64	H	-3.22234	11.19923	-0.80803
65	H	-2.79301	11.31107	1.620477
66	H	-7.23932	6.939374	5.478367
67	H	-5.33887	5.450325	4.874758
68	H	-3.19388	6.408632	4.148013
69	H	0.023266	8.368655	2.074095
70	H	1.887685	6.816383	2.499447
71	H	1.983568	5.522703	4.621792
72	H	0.1943	5.822887	6.326467
73	H	-1.66347	7.381666	5.91578
74	H	-2.48733	7.017772	1.753469
75	H	-2.94541	6.907348	-0.66285
76	H	-3.30648	8.998021	-1.96541
77	H	-3.82814	13.53876	6.046385
78	H	-5.3609	14.56415	7.694686
79	H	-4.45305	15.90914	9.58245
80	H	-1.99361	16.22156	9.798066
81	H	-0.46499	15.19661	8.166449
82	H	0.375791	16.20931	5.97872
83	H	0.585888	18.17394	4.51185
84	H	-0.40641	18.14446	2.228718
85	H	-1.63114	16.12475	1.44541
86	H	-1.87072	14.16485	2.926108
87	H	1.816266	14.07784	4.731805
88	H	4.035934	13.70196	5.72987
89	H	4.236737	12.82866	8.050525
90	H	2.178174	12.31585	9.353116
91	H	-0.04234	12.67838	8.360692
92	H	-4.32991	11.11905	7.148583
93	H	-4.16025	10.01694	9.396297
94	H	-1.95724	9.012346	10.06891
95	H	-0.01136	9.13658	8.489545

96	H	2.947871	8.726621	7.183657
97	H	5.280183	7.907945	7.302804
98	H	7.538566	7.689335	6.273763
99	H	9.080782	8.13454	4.389941
100	H	1.50538	10.65926	4.245654
101	H	5.955881	10.21691	2.285214
102	H	8.286891	9.399701	2.395144
103	H	3.708041	10.43114	3.314417

Table S21 Coordinates of optimized geometry of complex **3c**.

Tag	Symbol	X	Y	Z
1	Ru	9.092735	3.729457	9.635615
2	C	9.525676	2.00485	10.1663
3	O	9.843085	0.928326	10.47403
4	Cl	6.774672	3.724408	10.575
5	N	9.165876	5.774629	8.752804
6	C	8.510807	6.920844	8.533292
7	H	7.495336	6.971314	8.91318
8	C	9.096295	7.987565	7.860581
9	H	8.538747	8.903973	7.699768
10	C	10.42005	7.840828	7.401597
11	H	10.90106	8.659327	6.870775
12	C	11.11845	6.662738	7.619074
13	H	12.13576	6.513855	7.277983
14	C	10.45287	5.62647	8.314309
15	N	10.88204	4.389728	8.671343
16	N	12.12361	4.029612	8.324547
17	C	12.54314	2.848951	8.648296
18	H	11.87878	2.181934	9.193725
19	C	13.88733	2.389886	8.29657
20	C	14.73595	3.206644	7.552052
21	H	14.37154	4.18103	7.243303
22	C	16.03361	2.796982	7.191747
23	H	16.6628	3.466579	6.609914
24	C	16.50455	1.555433	7.568889
25	H	17.50547	1.232202	7.291525
26	C	15.68471	0.678169	8.326773
27	C	16.15952	-0.60512	8.720767
28	H	17.16531	-0.89727	8.425536
29	C	15.37295	-1.46254	9.457331
30	H	15.74971	-2.43937	9.750088
31	C	14.06707	-1.06511	9.834344
32	H	13.44395	-1.73861	10.4174
33	C	13.57629	0.171905	9.469079
34	H	12.57339	0.439295	9.781407
35	C	14.35752	1.087193	8.704695
36	C	9.428446	6.388234	12.15235
37	C	8.080332	6.750611	11.98317

38	H	7.369381	6.019757	11.60808
39	C	7.64782	8.037193	12.31007
40	H	6.600072	8.297657	12.1807
41	C	8.551638	8.984408	12.80123
42	H	8.213183	9.986812	13.05151
43	C	9.891465	8.63135	12.97425
44	H	10.60343	9.355953	13.36196
45	C	10.32742	7.340243	12.65789
46	H	11.36979	7.084734	12.81501
47	C	9.312498	3.79478	13.34966
48	C	8.541762	2.625581	13.32415
49	H	8.220102	2.205196	12.38085
50	C	8.143093	2.01229	14.51729
51	H	7.540588	1.108608	14.47659
52	C	8.504294	2.562206	15.74758
53	H	8.190988	2.086076	16.67337
54	C	9.264988	3.736447	15.78367
55	H	9.546006	4.178238	16.73644
56	C	9.662537	4.348316	14.59512
57	H	10.24933	5.261234	14.64076
58	C	11.73005	4.557305	11.96054
59	C	12.54656	5.452019	11.24735
60	H	12.10105	6.228191	10.63316
61	C	13.93707	5.350646	11.30871
62	H	14.55012	6.052526	10.7494
63	C	14.53747	4.340722	12.06591
64	H	15.6203	4.255221	12.10259
65	C	13.73623	3.433152	12.76147
66	H	14.19095	2.63564	13.34339
67	C	12.34337	3.540726	12.71138
68	H	11.73823	2.827873	13.26238
69	C	9.647698	2.608461	6.273652
70	C	10.09977	3.654939	5.453564
71	H	9.58909	4.613038	5.457742
72	C	11.20839	3.479654	4.622036
73	H	11.54024	4.301752	3.992737
74	C	11.88934	2.259764	4.602805
75	H	12.75325	2.124482	3.957435
76	C	11.46139	1.219124	5.430379
77	H	11.99322	0.271385	5.437803
78	C	10.3544	1.393865	6.264052
79	H	10.03986	0.573246	6.902423
80	C	7.035484	3.906267	6.532022
81	C	6.133309	4.707372	7.248563
82	H	6.186834	4.741795	8.331698
83	C	5.142615	5.431302	6.57815
84	H	4.448354	6.041824	7.150449
85	C	5.0404	5.369053	5.186801
86	H	4.271298	5.935302	4.667328

87	C	5.92975	4.566491	4.465916
88	H	5.856315	4.503622	3.382932
89	C	6.916191	3.836845	5.132844
90	H	7.593651	3.218163	4.553385
91	C	7.394566	1.223271	7.484582
92	C	6.80264	0.752027	8.664951
93	H	6.861997	1.341635	9.572781
94	C	6.10005	-0.45782	8.670966
95	H	5.64698	-0.80643	9.595463
96	C	5.977999	-1.20875	7.501016
97	H	5.433927	-2.14996	7.507938
98	C	6.556349	-0.74079	6.316016
99	H	6.463925	-1.31517	5.397531
100	C	7.254783	0.466968	6.306636
101	H	7.699343	0.811116	5.37787
102	P	9.890685	4.626987	11.79619
103	P	8.258583	2.865541	7.463695

Table S22 Coordinates of optimized geometry of complex **4b**.

Tag	Symbol	X	Y	Z
1	Ru	17.6559	11.84136	11.88437
2	C	17.87298	10.20385	12.70522
3	O	18.0206	9.191606	13.25803
4	Cl	16.83113	10.90411	9.728927
5	N	17.61708	14.11419	11.48505
6	C	17.42576	15.30567	10.80795
7	C	16.96713	15.46112	9.492546
8	H	16.72182	14.58443	8.902837
9	C	16.83806	16.74544	8.964303
10	H	16.48415	16.86716	7.943738
11	C	17.15737	17.88014	9.72559
12	H	17.04975	18.87202	9.295487
13	C	17.6164	17.74314	11.03964
14	H	17.86623	18.61861	11.63307
15	C	17.7466	16.46044	11.56842
16	S	18.30825	16.00632	13.18928
17	C	18.07053	14.3167	12.72189
18	N	18.27946	13.20463	13.42577
19	N	18.74803	13.32353	14.68058
20	C	18.95959	12.2452	15.3587
21	H	18.75904	11.26452	14.92031
22	C	19.47697	12.27914	16.72189
23	C	19.77436	13.51074	17.38469
24	H	19.60228	14.44032	16.85179
25	C	20.26928	13.5154	18.66517
26	H	20.49274	14.45915	19.15902
27	C	20.5027	12.30054	19.37573
28	C	21.01607	12.2756	20.69887

29	H	21.24051	13.21919	21.19214
30	C	21.22997	11.07858	21.35387
31	H	21.62344	11.07411	22.36714
32	C	20.93732	9.850881	20.70845
33	H	21.10898	8.913653	21.23178
34	C	20.43697	9.842627	19.42255
35	H	20.21217	8.900889	18.92611
36	C	20.20631	11.0593	18.72129
37	C	19.69494	11.08593	17.39722
38	H	19.47265	10.14066	16.90432
39	C	20.41992	12.78807	9.565835
40	C	19.44888	12.9927	8.574426
41	H	18.44846	12.59641	8.711019
42	C	19.77169	13.67884	7.400176
43	H	19.00766	13.82636	6.641047
44	C	21.06171	14.17459	7.202278
45	H	21.30809	14.71341	6.29077
46	C	22.03635	13.97186	8.183816
47	H	23.04549	14.35032	8.040566
48	C	21.72052	13.27881	9.354025
49	H	22.49324	13.13035	10.10107
50	C	21.18762	12.29953	12.3465
51	C	21.47495	13.66203	12.53002
52	H	21.04949	14.40594	11.8634
53	C	22.31068	14.08032	13.56761
54	H	22.51895	15.13988	13.69171
55	C	22.86756	13.14541	14.44426
56	H	23.51632	13.47142	15.25293
57	C	22.57304	11.78956	14.28307
58	H	22.98938	11.05457	14.96702
59	C	21.73459	11.37005	13.24716
60	H	21.51738	10.31137	13.13882
61	C	20.64601	10.09506	10.53168
62	C	22.02961	9.886518	10.38305
63	H	22.73159	10.68169	10.61431
64	C	22.52113	8.655717	9.947818
65	H	23.59377	8.511547	9.844558
66	C	21.63734	7.614072	9.64445
67	H	22.0203	6.654873	9.305015
68	C	20.26301	7.816622	9.775039
69	H	19.56596	7.01873	9.532335
70	C	19.76807	9.04969	10.21372
71	H	18.6974	9.204129	10.27493
72	C	14.13064	13.06508	11.86378
73	C	13.01052	13.61514	12.51253
74	H	12.86475	13.47041	13.57813
75	C	12.0726	14.36291	11.79841
76	H	11.21612	14.78584	12.31769
77	C	12.23315	14.56368	10.4239

78	H	11.50197	15.14501	9.867757
79	C	13.3367	14.01144	9.771426
80	H	13.46894	14.15801	8.702483
81	C	14.28247	13.26906	10.48466
82	H	15.1253	12.82711	9.964923
83	C	15.3032	12.55547	14.49793
84	C	15.26288	13.92751	14.79471
85	H	15.17138	14.65827	13.99677
86	C	15.33821	14.37191	16.11684
87	H	15.30611	15.43835	16.32467
88	C	15.46075	13.45422	17.16319
89	H	15.52063	13.80077	18.19153
90	C	15.51972	12.08791	16.87792
91	H	15.62857	11.36541	17.68256
92	C	15.44917	11.64224	15.55607
93	H	15.49858	10.57599	15.35429
94	C	14.36876	10.37084	12.829
95	C	13.23366	10.25734	13.65263
96	H	12.93518	11.08196	14.29245
97	C	12.48193	9.082195	13.67023
98	H	11.61093	9.01135	14.31707
99	C	12.84692	8.002393	12.85875
100	H	12.26094	7.086769	12.87254
101	C	13.96419	8.110603	12.02983
102	H	14.25288	7.282059	11.38824
103	C	14.72102	9.28723	12.01216
104	H	15.56629	9.368807	11.33873
105	P	19.99381	11.75508	11.04617
106	P	15.32575	11.96027	12.74977

Table S23 Physical characteristics

Parameters	Set-A			Set-B		
	RuH(CO)Cl(PPh ₃) ₃	3a	1a	RuH(CO)Cl(PPh ₃) ₃	4a	2a
pH	5.8	6.9	7.2	5.4	6.7	7.4
EC (in microsiemens)	243.42	367.16	174.37	275.19	326.43	228.96
Solubility in water	Sparsely soluble	Sparsely soluble	Completely soluble	Sparsely soluble	Sparsely soluble	Completely soluble
Solubility in ethanol	Sparsely soluble	Sparsely soluble	Sparsely soluble	Sparsely soluble	Sparsely soluble	Sparsely soluble
Solubility in DMSO	Completely soluble	Completely soluble	Completely soluble	Completely soluble	Completely soluble	Completely soluble

Table S24 Antimicrobial and antifungal assay: ZOI (in mm) produced by RuH(CO)Cl(PPh₃)₃, **1a**, **3a** (Set-A)

Microorganism	ZOI (in mm) produced by RuH(CO)Cl(PPh ₃) ₃ , 1a , 3a (Set-A)						
	Control (DMSO)	RuH(CO)Cl(PPh ₃) ₃	1a	3a	Tetracycline	Streptomycin	Ketoconazole
<i>Bacillus subtilis</i>	17±0.02	23±0.1		14±0.05	29±0.05	20.3±0.4	
<i>Bacillus megaterium</i>	12±0.12	13±0.16		4±0.06	17±0.15	21.7±0.9	
<i>Staphylococcus</i> spp.	3.5±0.05	7±0.06		1±0.01	5±0.01	24.2±0.8	
<i>Streptococcus</i> spp.	15±0.01	10±0.05		6±0.01	18±0.40	21.5±0.9	
<i>Klebsiella</i> spp.	9±0.04	12±0.05		3±0.04	14±0.05		24.3±0.5
<i>Pseudomonas</i> spp.	4±0.01	11±0.12		7±0.02	18±0.04		23.6±0.9
<i>E. coli</i>	7±0.15	15±0.12		5±0.04	16±0.01		22.4±1.1
<i>Malassezia</i> spp.	8±0.02	7±0.15		3±0.02	12±0.15		
<i>Alternaria</i> spp.	5±0.05	8±0.02		1±0.01	6±0.03		
<i>Aspergillus</i> spp.	3.5±0.05	2±0.01		1±0.02	8±0.02		

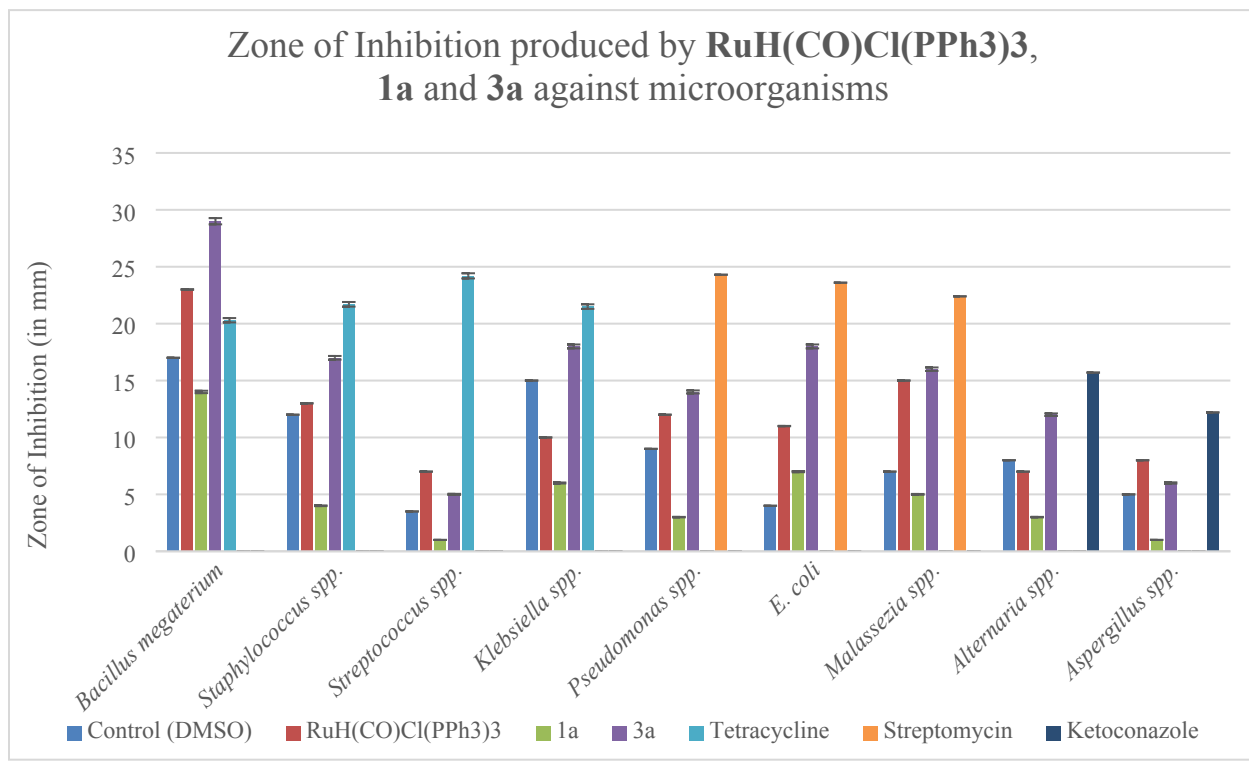


Fig. S19 Graph representing the zone of inhibition of **1a** the complex **3a** against the tested microorganisms.

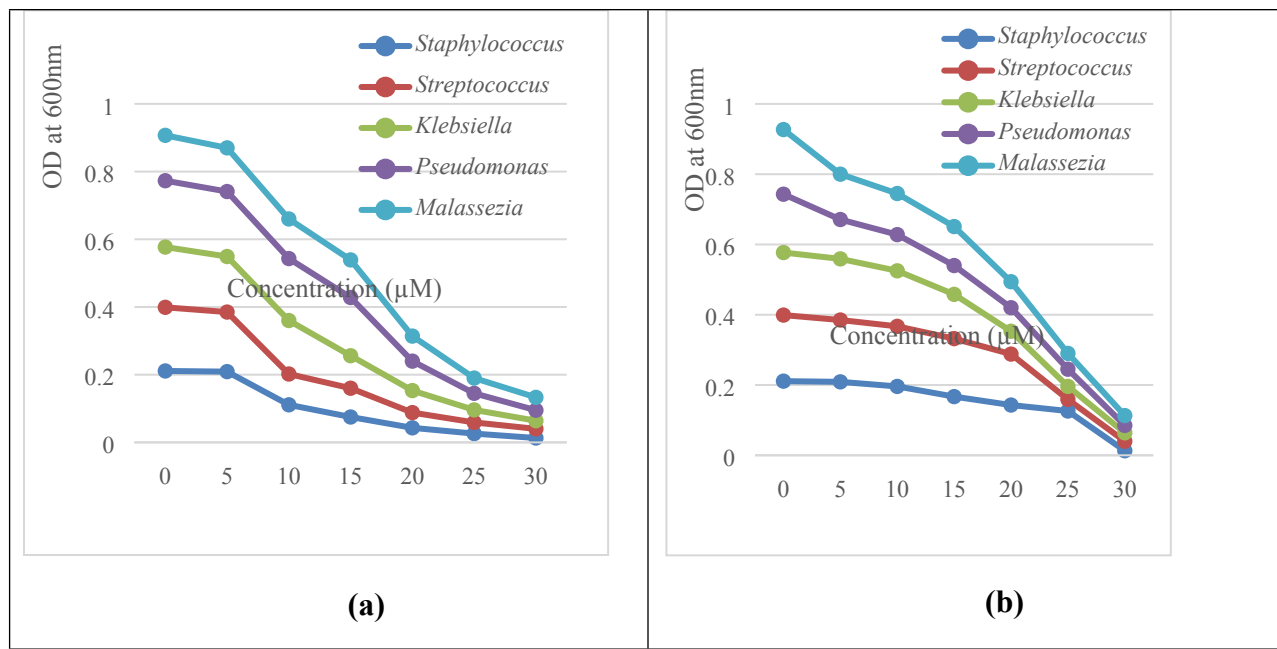


Fig. S20 Determination of MIC of (a) $\text{RuH}(\text{CO})\text{Cl}(\text{PPh}_3)_3$ and (b) **2a** against a few selected microorganisms by turbidimetric method.

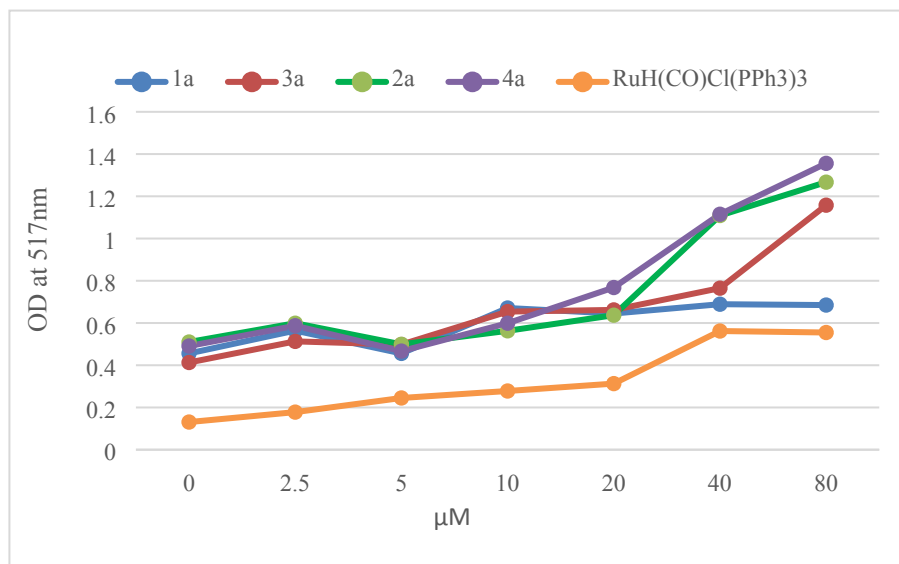


Fig. S21 DPPH radical scavenging exhibited activity by $\text{RuH}(\text{CO})\text{Cl}(\text{PPh}_3)_3$, **1a**, **3a**, **2a** and **4a**.

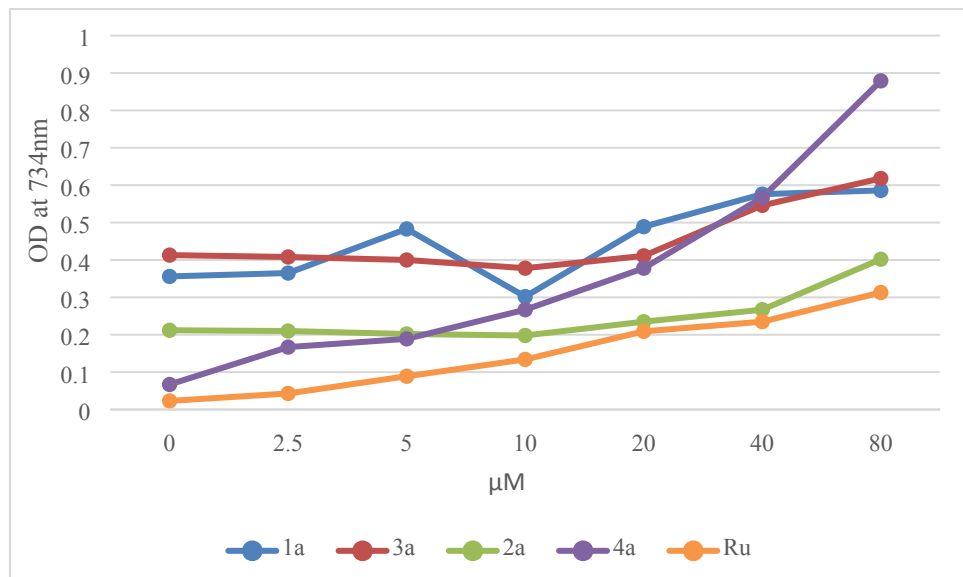


Fig. S22 ABTS radical scavenging activity exhibited by $\text{RuH}(\text{CO})\text{Cl}(\text{PPh}_3)_3$, **1a**, **3a**, **2a** and **4a**.

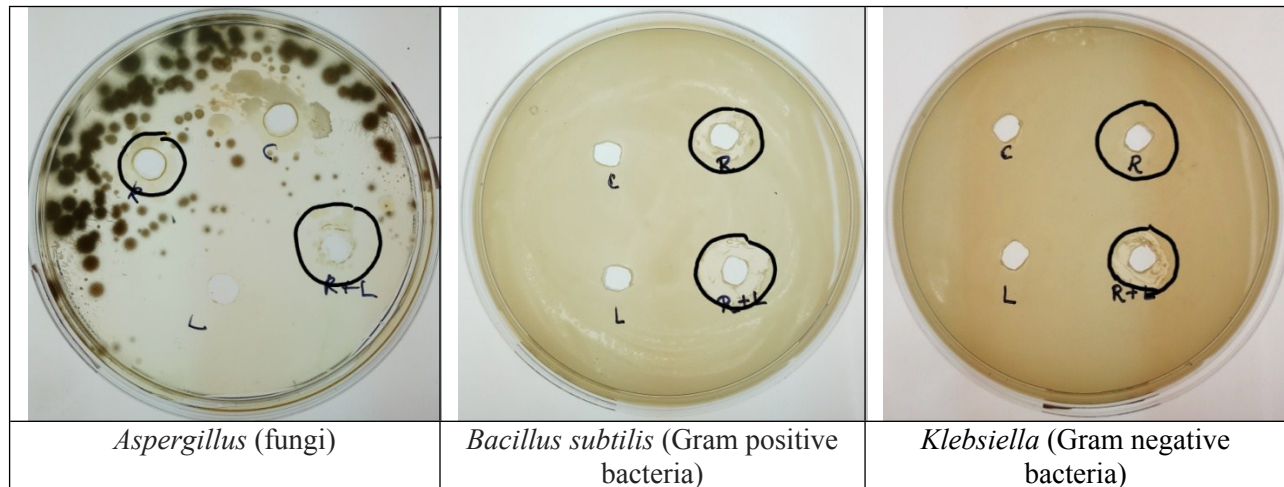


Fig. S23 ZOI when the microorganisms were treated with the set containing **2a** and **4a** (abbreviations were used: C : Solvent control (DMSO), R: $\text{RuH}(\text{CO})\text{Cl}(\text{PPh}_3)_3$, L: **2a** and R+L : **4a**).

References:

1. R. L. Martin, *J. Chem. Phys.*, 2003, **118**, 4775–4777.